Received: 2 March 2024 | Revised: 21 June 2024 | Accepted: 21 June 2024

DOI: 10.1111/gcb.17414

Global Change Biology WILEY

RESEARCH ARTICLE

Pushed waves, trailing edges, and extreme events: Eco-evolutionary dynamics of a geographic range shift in the owl limpet, *Lottia gigantea*

Erica S. Nielsen[1] | Samuel Walkes[1,2] | Jacqueline L. Sones[3] | Phillip B. Fenberg[4] | David A. Paz-García[5] | Brenda B. Cameron[1] | Richard K. Grosberg[1] | Eric Sanford[1,2] | Rachael A. Bay[1]

[1]Department of Evolution and Ecology, University of California Davis, Davis, California, USA

[2]Bodega Marine Laboratory, University of California Davis, Bodega Bay, California, USA

[3]Bodega Marine Reserve, University of California Davis, Bodega Bay, California, USA

[4]School of Ocean and Earth Sciences, National Oceanography Centre Southampton, University of Southampton, Southampton, UK

[5]Laboratorio de Genética para la Conservación, Centro de Investigaciones Biológicas del Noroeste (CIBNOR), La Paz, Baja California Sur, Mexico

Correspondence
Erica S. Nielsen, Department of Evolution and Ecology, University of California Davis, Davis, CA 95616, USA.
Email: erica.nielsen@tnc.org

Funding information
National Science Foundation, Grant/Award Number: OCE-2023297 and OCE-2322845

Abstract

As climatic variation re-shapes global biodiversity, understanding eco-evolutionary feedbacks during species range shifts is of increasing importance. Theory on range expansions distinguishes between two different forms: "pulled" and "pushed" waves. Pulled waves occur when the source of the expansion comes from low-density peripheral populations, while pushed waves occur when recruitment to the expanding edge is supplied by high-density populations closer to the species' core. How extreme events shape pushed/pulled wave expansion events, as well as trailing-edge declines/contractions, remains largely unexplored. We examined eco-evolutionary responses of a marine invertebrate (the owl limpet, *Lottia gigantea*) that increased in abundance during the 2014–2016 marine heatwaves near the poleward edge of its geographic range in the northeastern Pacific. We used whole-genome sequencing from 19 populations across >11 degrees of latitude to characterize genomic variation, gene flow, and demographic histories across the species' range. We estimated present-day dispersal potential and past climatic stability to identify how contemporary and historical seascape features shape genomic characteristics. Consistent with expectations of a pushed wave, we found little genomic differentiation between core and leading-edge populations, and higher genomic diversity at range edges. A large and well-mixed population in the northern edge of the species' range is likely a result of ocean current anomalies increasing larval settlement and high-dispersal potential across biogeographic boundaries. Trailing-edge populations have higher differentiation from core populations, possibly driven by local selection and limited gene flow, as well as high genomic diversity likely as a result of climatic stability during the Last Glacial Maximum. Our findings suggest that extreme events can drive poleward range expansions that carry the adaptive potential of core populations, while also cautioning that trailing-edge extirpations may threaten unique evolutionary variation. This work highlights the importance of understanding how both trailing and leading edges respond to global change and extreme events.

KEYWORDS
demographic history, eco-evolutionary, gene flow, genomic variation, larval simulation, population assignment, species distribution models

1 | INTRODUCTION

As climate change increasingly alters marine environments, many species are shifting poleward (Bates et al., 2014; Burrows et al., 2011; Sunday et al., 2012). Poleward range expansions often reflect organisms tracking their thermal niches, especially in marine species that shift at faster rates than their terrestrial counterparts (Pinsky et al., 2020; Poloczanska et al., 2013). However, ecological niche models do not always accurately predict the dynamics of a species' geographic range, in part because intraspecific genomic and phenotypic variation can lead to different expansion success depending on the source populations of recruitment (Bestion et al., 2015; Hastings et al., 2020). A growing body of theoretical work on eco-evolutionary feedbacks of range expansions (Andrade-Restrepo et al., 2019; Henry et al., 2013; Legrand et al., 2017; Norberg et al., 2012) suggests that the expanding edge is likely to harbor distinct frequencies of alleles or fixed mutations due to genetic drift following a bottleneck event (which are often associated with range expansions), or driven by low gene flow and/or local adaptation to the novel range edge environment (Hardie & Hutchings, 2010; Williams et al., 2019). The genomic composition of the leading edge will depend on the expansion history and the environmental drivers of the range shift.

Broadly, range expansions can be described as "pulled" or "pushed" waves (Figure 1; Miller et al., 2020; Williams et al., 2019). Pulled waves occur when the source of the expansion comes from high-fitness, low-density peripheral populations being "pulled" by small leading-edge founding populations with higher dispersal or reproductive capacity (Miller et al., 2020). In contrast, pushed waves are characterized by low-fitness peripheral populations, when recruitment to the expanding edge is supplied by high-density populations closer to the species' core (Miller et al., 2020). Because in pulled waves recruitment is mainly from the pre-existing range edge, evolutionary consequences can include the expansion front having lower genetic diversity, unique allele frequencies due to allele surfing, greater numbers of private alleles, and genomic differentiation from the core (Garnier & Lewis, 2016; Hallatschek & Nelson, 2008). Conversely, pushed wave recruits represent a larger gene pool as they originate from high-density populations across a broader spatial extent than pulled wave expansions driven by previous range edges. Thus, pushed wave expansion fronts should have higher genetic diversity, higher genetic load, and less genomic differentiation from the core of the species' range compared with pulled waves (Bonnefon et al., 2014; Szűcs et al., 2019). The mechanism of range expansion can in turn affect the expansion rate. Pulled waves can experience a positive feedback of spatial sorting aggregating strong dispersers at the range edge which then escape from density-dependent competition, leading to "spatial selection" for high-dispersal ability, thereby accelerating range expansions; pushed waves can experience a feedback of maladaptation to novel conditions counteracting dispersal selection, decelerating the rate of expansion (Andrade-Restrepo et al., 2019; Miller et al., 2020). Determining whether range expansions occurred via pushed or pulled waves can help predict future species' shifts and their ecological consequences (Kerr, 2020).

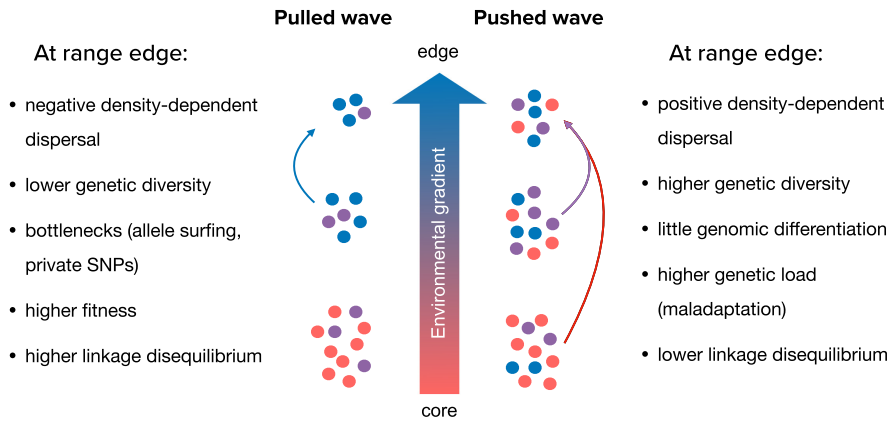

FIGURE 1 Conceptual diagram of pulled and pushed wave range expansions and genetic outcomes. Individual genotypes are represented by the different colored circles, with higher fitness alleles matching the color along the environmental gradient. The left demonstrates a pulled wave: Where the expansion is "pulled" typically by high-dispersal/high-fitness individuals from the pre-existing range-edge population. As the edge populations in pulled waves are likely small and negative density dependent, they will often experience spatial sorting, genetic drift, allele surfing, and have lower genetic diversity and higher linkage disequilibrium. The right shows a pushed wave: Where the expansion is "pushed" by high-density populations well behind the leading edge. This type of expansion is usually characterized by positive density dependence in growth/dispersal, with the leading edge showing higher genetic diversity and maladaptation, as well as lower genetic differentiation from the core.

Few studies have empirically assessed the evolutionary dynamics of poleward marine range shifts (Banks et al., 2010; Dawson et al., 2010; Fifer et al., 2022; Hu & Dong, 2022; Ramos et al., 2018; Wang et al., 2022). Of the studies that have tested for genetic differentiation in marine species experiencing poleward expansions, several have identified the expanded population as a distinct evolutionary unit (Fifer et al., 2022; Ramos et al., 2018; Wang et al., 2022), likely driven by novel selective forces and genetic bottlenecks from founder effects. Studies have predominantly focused on range expansions driven by long-term climatic warming rather than those initiated during extreme events. Pulled and pushed waves, and range expansions as a whole, can occur over short timeframes (Burford et al., 2022), as well as with ocean currents flowing against the direction of climatic velocities (García Molinos et al., 2022). Shorter-term warming caused by extreme events, such as marine heatwaves (MHWs), can rapidly shift the distribution and abundance of marine species (Lonhart et al., 2019; Sanford et al., 2019), accelerate existing poleward range shifts (Smith et al., 2019), and cause "genetic tropicalization" within species in which warm-adapted alleles rapidly replace cool-adapted ones (Coleman et al., 2020). The evolutionary imprint of an extreme event may differ from that of gradual warming, as the selection forces are likely to be stronger and more acute (Harvey et al., 2022; Marzonie et al., 2023). Additionally, El Niños and other MHWs may also cause wind and ocean current anomalies (Fewings & Brown, 2019; Li et al., 2022; Sanford et al., 2019), which are likely to influence dispersal, spatial sorting, and subsequent eco-evolutionary feedbacks. As climate anomalies are projected to increase in frequency and severity (Oliver et al., 2018), understanding how these extreme events shape evolutionary trajectories of range-shifting species is critical.

Here, we explore eco-evolutionary dynamics of a recent range expansion of the owl limpet, *Lottia gigantea*. This marine gastropod increased in abundance within its northern edge populations in association with the 2014–2016 MHWs (resulting from the warm-water blob and 2015–2016 El Niño) along the Eastern Pacific (Sanford et al., 2019; hereafter referred to as the "MHWs"). This region of expansion (Figure 2a) has seen ongoing recruitment for the first time in over 15 years of monitoring (Fenberg & Rivadeneira, 2011; Sanford et al., 2019), which highlights the novelty of this particularly strong and prolonged extreme event (Sen Gupta et al., 2020). The species' range historically extended even farther north, with specimens existing from ca. 41.7°N, compared with the ca. 39.4°N of the current range edge (Fenberg & Rivadeneira, 2011). However, there are no known occurrences within this historical range since the early 1960s (including surveys conducted by the authors in seven separate visits from 2003 to 2022). Biogeographic analyses suggest that the northern edge of the distribution is recruitment-limited, while the southern edge is habitat-limited (Fenberg & Rivadeneira, 2011). A previous study using microsatellite markers revealed no significant structure across the California range of *L. gigantea* (Fenberg et al., 2010). This system provides the ideal backdrop to explore range expansion dynamics in a pulled vs. pushed wave framework, as genomic imprints of the range shift may become diluted by future demographic changes and selection over time.

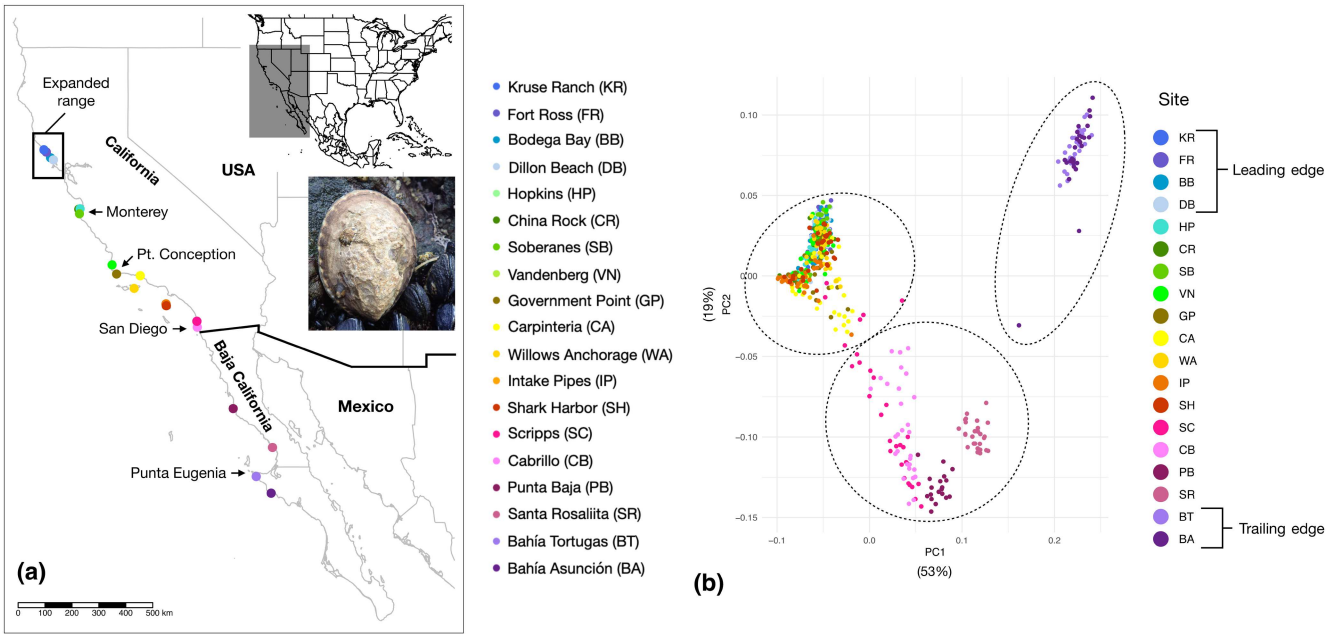

FIGURE 2 Sampling sites and population clustering. (a) Map of *Lottia gigantea* sample sites for genomic sequencing (Table S1) along the Pacific coast of North America, with the expanded range (where increased recruitment occurred in association with marine heatwaves) highlighted by the black box. Locations of common phylogeographic breaks (Monterey Bay, Point Conception, San Diego, and Punta Eugenia) are also indicated with arrows. (b) The first and second components of a principal components analysis (PCA) of SNP data with individuals colored by site, and the three clusters identified by the Kmeans clustering analysis encircled by dashed lines. Leading- and trailing-edge populations are based on abundance trends from Fenberg and Rivadeneira (2011).

We leverage whole-genome sequencing data to characterize population substructure, genomic diversity, and differentiation across the species' range, as well as identify source populations for the recent recruitment event. We address the following questions: (1) What demographic changes in migration, distribution, and effective population size of *L. gigantea* populations have occurred, and how have historical and recent shifts in abundance shaped genomic variation at the range edges? (2) Do the recent heatwave-mediated recruitment events represent a pushed or pulled wave? and (3) How do patterns of gene flow and dispersal influence evolutionary trajectories of the leading-edge, core, and trailing-edge populations? These patterns can be used to understand how long-term warming and extreme events interact to influence the demographic and genetic attributes of leading- and trailing-edge populations, and their potential for future range expansion and contraction.

2 | METHODS

2.1 | Study system, sampling, and sequencing

We sampled 19 sites on the Pacific coast of North America, spanning most of the contemporary range of *L. gigantea* (Figure 2; Table S1). *Lottia gigantea* is a broadcast spawner, with gamete release occurring during the northern hemisphere winter (November–February; Daly, 1975; Sanford et al., unpublished data). They have lecithotrophic larvae, with a pelagic larval duration of ca. 4–21 days at 12–18°C (Sanford et al., unpublished data). *Lottia gigantea* are protandric hermaphrodites, changing sex from male to female as they grow (Fenberg & Roy, 2012; Kido & Murray, 2003). As grazers, they play a key role in regulating available space within the rocky intertidal zone and influence the abundance of other sessile invertebrates such as barnacles, mussels, and anemones (Lindberg et al., 1998; Stimson, 1970). Human exploitation of *L. gigantea* also occurs within most of the species' range, with size-selective harvesting leading to differences in growth rates, size at sex change, and abundance (Fenberg & Roy, 2012; Sagarin et al., 2007).

Sampling occurred from November 2020 to January 2022. We non-lethally excised a small piece of foot muscle tissue (Table S1). For all locations except the four northern sites, we collected tissue from roughly 30 individuals per site, comprised of 10 individuals within each of the following size ranges: 10–25 mm (small), 30–40 mm (medium), and >40 mm (large). Sampling of the four northern sites (i.e., expanded range) also consisted of roughly 10 small, medium, and large individuals per site. However, as individual limpets at these four sites have been closely monitored over the past 8 years, these sites had known cohorts based on the estimated year of settlement. Size classes at sites for which we do not have monitoring data were chosen based on our data and previous growth curves (Kido & Murray, 2003) to approximately group individuals into those that settled during the MHWs, soon after the MHWs (late 2016 or late 2017), or well after the MHWs (late 2018 or late 2019). For our purposes, we group these individuals into those that settled during or after the MHWs. Tissue was stored in 90% ethanol at −20°C. We used the Qiagen DNAeasy extraction kit to perform DNA extractions following the manufacturer's protocols. DNA quantity and quality were assessed with Nanodrop, Qubit, and gel electrophoresis. Library preparation followed the Nextera Lite protocol, with adaptations following Rowan et al. (2019). Briefly, this consisted of normalizing samples, tagmentation, PCR, pooling samples, and bead size selection. The purified samples were run on a High Sensitivity DNA Bioanalyzer chip and then sent to BGI Genomics for whole-genome sequencing on the DNBSEQ-T7 PE150 platform on four lanes of sequencing.

2.2 | Bioinformatic processing and SNP calling

We used fastQC to assess the overall quality of raw reads. Initially quality and adapter filtering were performed with fastp (Chen et al., 2018). Quality-filtered reads were mapped onto the *L. gigantea* reference genome using BWA-MEM (NCBI RefSeq assembly GCF_000327385.1; Li, 2013). Mapped reads were filtered (with parameters -q 20 -f 2 -F 8 -F 4), sorted, indexed, and converted to bam files using samtools v1.8 (Li et al., 2009). We removed duplicate reads with picard v1.119 MarkDuplicates (http://broadinstitute.github.io/picard/), soft-clipped overlapping reads with the clipOverlap function bamUtils v1.0.14 (Breese & Liu, 2013), and realigned insertions/deletions with GATK v3 RealignerTargetCreator and IndelRealigner (McKenna et al., 2010). Due to variable sequencing and coverage across samples (Figure S1–S3), we chose to call single-nucleotide polymorphisms (SNPs) and estimate genotype likelihoods with the Analysis of Next Generation Sequencing Data software (ANGSD) v0.931 (Korneliussen et al., 2014). Genotype likelihoods were estimated simulating the GATK method (−GL 2), using the most frequent as the major allele (−doMajorMinor 1), and with the following parameters: -remove_bads 1 -baq 1 -skipTriallelic 1 -SNP_pval 1e-6 -uniqueOnly 1 -only_proper_pairs 1 -minMapQ 30 -minQ 20 -minMaf 0.05. In the same SNP-calling step, we filtered to only include SNPs that were present in at least 50% of individuals, and a total coverage below 3X the number of individuals. Using plink, we filtered SNPs that were in linkage disequilibrium (LD), using a r^2 of 0.5, with a window of 25kbp and step of 10kbp.

2.3 | Population structure and genomic variation

We used analyses of population structure to test whether the leading and trailing edges had higher levels of differentiation compared with the species' core. We ran principal components analyses (PCAs) with pcangsd v0.985 (Meisner et al., 2021) using the BEAGLE file from ANGSD. To identify clusters within the PCA, we ran the "kmeans" function in the R stats package. We created structure plots using NGSadmix, testing clusters (K) 1–10. We generated global-weighted pairwise F_{ST} values using unfolded two-dimensional site frequency spectrums (2dSFSs) created

with ANGSD. Sliding window F_{ST} was calculated over 25 kb non-overlapping windows with a step size of 5 kb. To further characterize population differentiation, we estimated covariance (Ω) matrices from allele frequencies in BayPass v.2.1 (Gautier, 2015). We ran BayPass with default parameters and then converted Ω to a correlation matrix with the cov2corr function of the R stats package.

We calculated several measures of genomic diversity, including expected heterozygosity (H_E), Watterson's theta (θW; Watterson, 1975), and nucleotide diversity (π; Nei, 1987). We calculated individual heterozygosity and averaged per population with ANGSD, which calculates the proportion of heterozygous genotypes (over the whole genome, excluding regions of low confidence) divided by the adjusted genome size. Heterozygosity was calculated from genotype likelihoods using the expectation maximization (EM) algorithm in ANGSD's realSFS using the following script: git@github.com:sbarfield/yap_ahyacinthus-.git/heterozygosity_beagle.r. To determine whether genomic diversity differed between different size classes, we also generated per-site H_E values for either the large individuals or small/medium individuals (small and medium individuals were grouped together here as they are both likely to have settled after the MHWs). θW and Tajima's D were calculated using ANGSD's realSFS, doThetas, and thetaStat, using the same parameters used for pairwise F_{ST} calculations. Nucleotide diversity was calculated from the ANGSD.geno file using the get.snpR.stats function of the snpR R package (Hemstrom & Jones, 2023). ANGSD has been shown to produce slightly higher π estimates compared with other methods such as pixy and VCFtools (Korunes & Samuk, 2021) but was chosen as it is more suitable for low and uneven coverage data (Korneliussen et al., 2014).

To assess the eco-evolutionary consequences of the expansion, we characterized genetic load, allele surfing/genetic drift, private alleles, and inbreeding at the expansion front compared with the core and trailing-edge populations. Estimates of genetic load were assessed with purifying selection, calculated as the ratio of the diversity at nonsynonymous vs. synonymous sites (θN/θS; Fifer et al., 2022). The type of mutation was identified using ensembl's variant effect predictor (McLaren et al., 2016), and then, θW was calculated from either subset of SNPs following the same procedure stated above. This analysis assumes that populations with higher diversity at nonsynonymous sites are experiencing purifying selection and have lower genetic load. To characterize the extent of allele surfing or genetic drift, we calculated the minor allele in the highest frequency (MAHF; Wilde et al., 2021). This metric consisted of the count of minor alleles that exist at their highest frequency in each population. The number of private alleles was calculated with the calc_private function of snpR. Inbreeding coefficients (F), here defined as the proportion of loci for an individual where the observed alleles are identical by descent, were estimated using ngsF v.1.2.0 (Vieira et al., 2016). Using genotype likelihoods from ANGSD, we ran the approximated expectation–maximization (EM) algorithm (–approx_EM), and then, the full EM maximum likelihood model. Inbreeding coefficients were then averaged across all individuals per site.

2.4 | Gene flow

We characterized patterns of gene flow across the species' range to investigate how ocean currents and larval dispersal within recent years may have shaped patterns of genomic variation. Isolation-by-distance (IBD) was generated using $F_{ST}/(1\text{-}F_{ST})$ as the pairwise genetic distance response variable and distance along the coastline (or Euclidean distance to island sites) calculated in QGIS as the explanatory variable. We assessed IBD with Mantel tests within the ecodist R package (Goslee & Urban, 2007) using 1000 permutations, and determined model significance with q-values generated by the q-value R package, using a false discovery rate (FDR) of 0.05. We visualized patterns of gene flow with fast estimated effective migration surfaces (FEEMS; Marcus et al., 2021). This method is similar to EEMS (Petkova et al., 2016), using a stepping-stone model to estimate migration within a user-defined grid, but also integrates a Gaussian Markov Random Field model for more efficient optimization. FEEMs was run with a lambda of 0.75, which we chose after running a leave-one-out cross-validation following the cross-validation.ipynb.

To investigate how larval dispersal influences patterns of gene flow, we ran larval simulation models with Opendrift v.1.71 (Dagestad et al., 2017), which is a Lagrangian particle tracking framework that calculates particle drift over a domain. Simulations were run separately, sourcing the larvae from predefined groupings based on the biogeographic regions defined in Blanchette et al. (2008). Separate models were run per grouping using minimum and maximum settlement age parameters guided by preliminary larval rearing experiments at either 18 or 12°C (Sanford et al., unpublished data). Models were run yearly during winter spawning months from 2012 to 2020. We used the available "BivalveLarvae" sub-model (https://github.com/simonweppe/opendrift/blob/master/opendrift/models/bivalvelarvae.py), which was built for the transport of pelagic ichthyoplankton, to include the larval behavior parameters of minimum and maximum age of settlement, as well as interactions with a coastline. Models were based on the "GLOBAL_MULTIYEAR_PHY_001_030," "WIND_GLO_WIND_L3_REP_OBSERVATIONS_012_005" reanalysis of the NEMO global ocean circulation model from 1992 to the present, at a 0.083°×0.083° spatial resolution (https://marine.copernicus.eu/access-data). These environmental inputs consisted of daily means of sea water velocities, mixed layer depths, wave heights, and wind velocities. Full Opendrift larval simulation methods can be found in the Supporting Information Methods.

2.5 | Population assignment

We used population assignment tests to assess the eco-evolutionary dynamics of the northern range edge, and whether recruitment dynamics support a pulled or pushed wave event. We ran Guided

Regularized Random Forest (GRRF) models (Deng & Runger, 2013) to assign source locations to recruits that arrived in the expanded range either during or following the MHWs. GRRFs are based on Random Forest (RF) models, which use supervised machine learning algorithms to create a series of decision trees to classify a set of features, which were SNPs in our analyses. The SNPs identified by the GRRFs represent genomic distinctions between source populations and are used to assign "unknown" individuals (i.e., recruits in the leading edge) to the different sources. The full description of the GRRF models can be found in the Supporting Information Methods. Two sets of population assignment tests were performed: assigning individuals from the expanded range which arrived (1) during the MHWs or (2) after the MHWs (based on yearly monitoring of individual limpets in the four northernmost sites). Population assignment tests used predefined geographic regions (based on Blanchette et al., 2008) as potential source populations. We did not include Mexico sites as source locations because larval simulation model outputs suggested limited gene flow between Mexico and California (see Section 3).

2.6 | Population demography

To disentangle whether genomic diversity and population structure are driven by historical or recent evolutionary processes, we simulated past demographic histories per genomic cluster. We used the Moments pipeline (Jouganous et al., 2017) to fit and compare predefined two-population past demographic models from 2dSFSs. To determine whether the leading edge has a distinct demographic history from the core populations, we ran multi-model inferences comparing the expanded range ("Leading-edge") with the genomically derived central California cluster ("Core_cluster"). We also compared demographic estimates of the southern genomic groupings: "Baja_cluster" and "South_cluster." All two-population folded models were run on 10 bootstrapped unfolded 2dSFSs, with six replicates per model. Models were evaluated based on their Akaike Information Criterion (AIC) values. We bootstrapped the best model 100 times over six replicates to estimate demographic parameters such as effective population size (N_e) and migration rates. We also generated stairway plots displaying the changes in N_e over time per each of the four groupings within the Moments analysis, using the unsupervised approach of StairwayPlot 2 (Liu & Fu, 2020). For both Moments and StairwayPlot analyses, we used a generation time of 2 years and a mutation rate of $1.6 \times 10{-}9$ (Chen et al., 2022). To further explore population recombination history and effective population sizes, we generated measures of LD decay from plink, and r^2 values were plotted with the following custom script: https://github.com/speciationgenomics/scripts/blob/master/ld_decay_calc.py. We ran StairwayPlot 2 and LD decay on the four northern "Leading-edge" sites to assess whether there are fine-scale differences within the expanded range.

2.7 | Past climatic suitability

To understand how historical climatic variation contributes to contemporary distributions of genetic variation, we conducted species distribution models (SDMs) to hindcast *L. gigantea* distribution from the present day to the Last Glacial Maximum (LGM) 21 thousand years ago (kya). The SDMs included mean sea surface temperature (SST) and sea surface salinity (SSS), and minimum air temperature (Tmin) as predictor variables. We only included contemporary occurrence points, excluding range edge regions where the species was present but not within the timeframe of the environmental predictor variables within the model (2000–2014). For detailed methods on SDMs, see Supporting Information Methods.

3 | RESULTS

3.1 | SNP identification and population structure

The number of raw reads, reads passing filters, and read depth varied across samples, with Intake Pipes (IP) having the lowest, and China Rock (CR) having the highest values across all three (Figures S1–S3). A total of 3,209,370 SNPs were identified by ANGSD, which was reduced to 908,948 SNPs after filtering for LD. These SNPs show population structuring, with a clear separation between the two southernmost sites (BT and BA; "South_cluster") and the rest of the range (Figure 2b). Additional sub-structuring was found with the two southernmost California sites and the two northern Mexico sites (the "Baja_cluster") separating from the rest of the California sites ("Core_cluster"; Figure 2b). The PCA of just the California sites shows some separation between the two southernmost sites (SC, CB) along PC2, which captures 18% of the variation, and no clustering among the rest of the sites (Figure S4). The K-means clustering analysis identified three clusters (Figure 2b), while the NGSadmix analysis identified $K=2$ as the best representation of clustering (Figure 3a). Hierarchical admixture plots show three clusters: two southernmost sites (BA, BT), followed by the four southern sites (SC, CB, PB, and SR), and the rest of the sites as a single cluster (Figure 3a,b; Figure S5). Differentiation among populations was low, with pairwise F_{ST} values ranging from 0.007 to 0.024. There was no evidence of significant IBD among sites (Mantel tests, p-value = .523, $R^2 = -.018$, Figure 3c).

3.2 | Range-wide genomic variation

Both leading and trailing edges showed high levels of genetic diversity, with the trailing edge exhibiting the highest levels of genomic load and drift. Genomic diversity varied across sites, with H_E, π, and θW all showing higher diversity at the range edges (Figure 4; Figure S6). Patterns of diversity across the range were similar between the small/medium and large individuals (Figure 4a). Tajima's

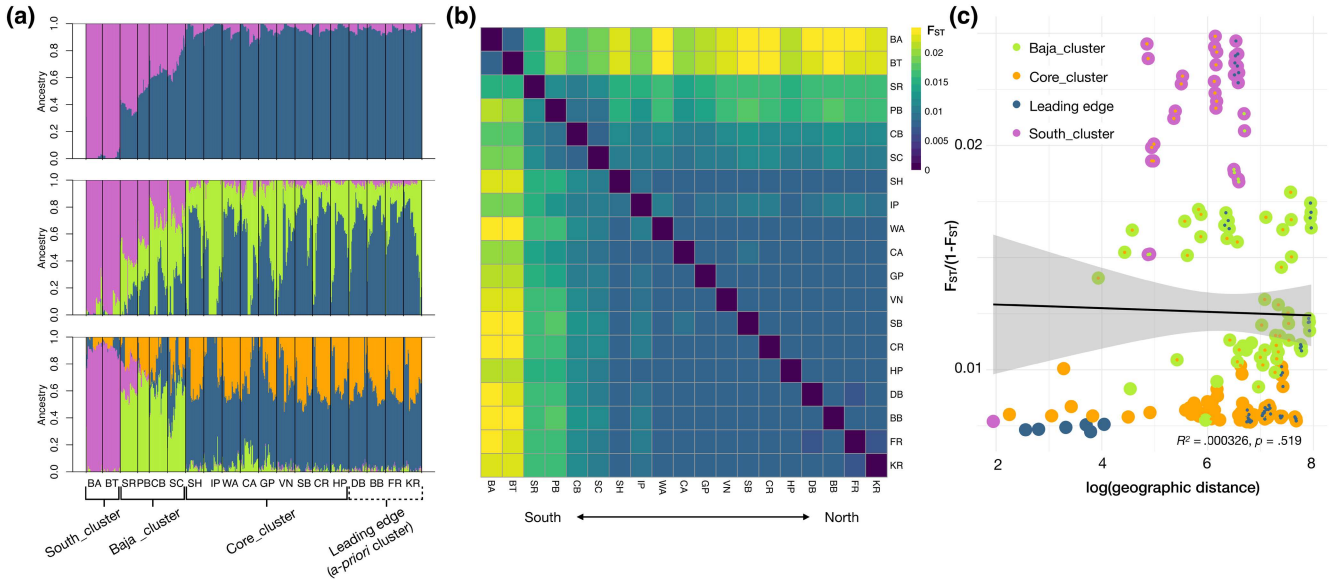

FIGURE 3 Population structure and genomic differentiation in *Lottia gigantea*. (a) Hierarchical clustering structure plots showing the percent ancestry for each individual from one of $K=2$ to $K=4$ groups (represented by the two to four different colors in plots). Genomically defined groupings are labeled on the x-axis with solid lines, and the predefined Leading-edge group is labeled with dashed lines. (b) Heatmap portraying pairwise F_{ST} values from the linkage disequilibrium (LD)-filtered SNP dataset. Site abbreviations are defined in Figure 2a. (c) The log of the geographic distance between sites and weighted pairwise F_{ST} values, with points colored by the outer and inner circles representing the clusters of the two sample sites being compared.

D was negative across all sites, with overall higher values at the range edges (Figure S6). Genetic load, represented by the diversity of nonsynonymous over synonymous SNPs ($\theta N/\theta S$), was highest in the trailing edge, followed by the northern range (Figure 4c). Minor alleles in highest frequency (MAHF) suggest that genetic drift or allele surfing is strong in southern populations (Figure 4d). The number of private SNPs was significantly higher in lower latitude sites, with Punta Baja (PB) having the highest and Willows Anchorage (WA) having the lowest number of private SNPs (p-value = .0021, adj $R^2 = .4208$). Range edges generally had lower inbreeding estimates (except for KR), and Intake Pipes had the highest inbreeding estimate (Figure S7).

3.3 | Patterns of gene flow and dispersal

Larval simulations support northward migration during MHW years. Similar settlement density patterns were found from larval simulations using parameters based on larvae reared at either 12 or 18°C, with varied larval dispersion estimates across years under both temperatures (Figure 5a, Figures S8 and S9). The years with heatwave anomalies, 2014–2016, as well as 2018–2020 (Weber et al., 2021; Wei et al., 2021), show noticeable increases in settlement densities farther north across the California-seeded regions (Figure 5a; Figures S8 and S9). The simulations also show Monterey-seeded larvae stranding within the extended range predominantly in the winters of 2018/2019 and 2019/2020 (Figure 5a), suggesting that these could be important years of recruitment within the four northern sites. The Opendrift analyses also show low settlement of Mexico-seeded larvae into California (Figure 5a). The FEEMs output suggests that there are significant breaks in gene flow around Punta Eugenia, San Diego, and Point Conception (Figure 5b).

Assignment tests suggest mixed recruitment from source populations across the species' core combined with ongoing local recruitment at the leading edge. Models assigning individuals that settled during the MHWs suggest that they came from all three predefined regions, and that there is no decrease in southern-sourced recruits as settlement-site latitude increases (Figure 6e,h). Models assigning individuals arriving after the MHWs reported fewer assignments from central and southern core sites (Figure 6f,i). The assignment tests suggest that self-recruitment is higher in the more northern leading-edge sites (FR and KR; Figure 6i). The GRRF models assigning individuals that settled after the MHWs also did not show an increase in southern-sourced recruitment within the leading-edge sites at lower latitudes (Figure 6f,i).

3.4 | Historical changes in demography and distribution

All genomic clusters display concordant demographic histories with broadly similar trends in population size over time and LD decay. LD decay was lower in the core populations (Core_cluster and Baja_cluster). Genome-wide LD was highest in the southern edge (South_cluster; Figure 7a). Present-day N_e was similar across regions, albeit with the expanded-range population having slightly lower N_e (Figure 7e). The four regions had similar changes in N_e over time, with two major decreases in N_e over the past 100 kya (Figure 7e). The Core_cluster had slightly different timing of population changes, with decreases

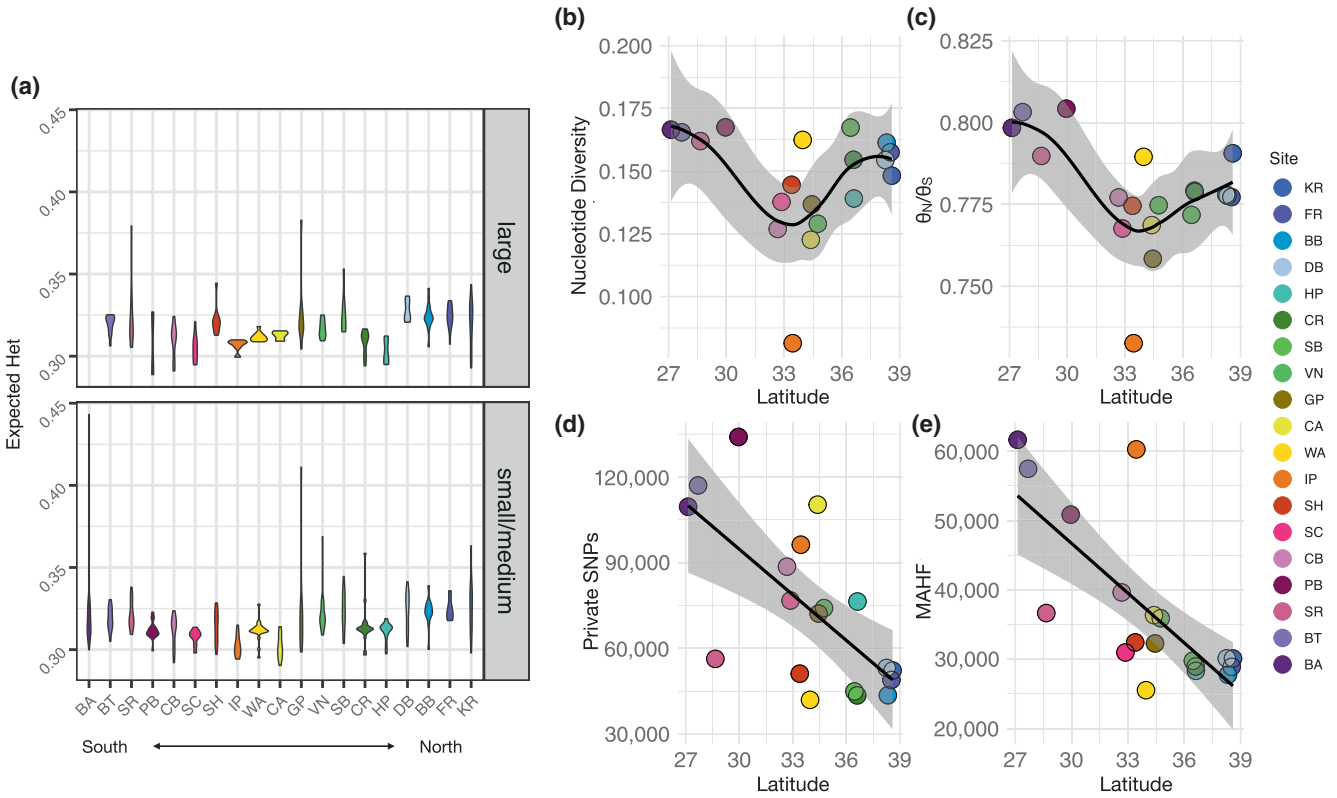

FIGURE 4 Range-wide genomic variation in *Lottia gigantea*. (a) Per-site genomic diversity (H_E; "Expected Het") is shown for both large (>40 mm; top panel) and small/medium (10–40 mm; bottom panel) individuals (as small/medium individuals are more likely to have settled after the MHWs). (b) Nucleotide diversity, (c) mutational load (estimated from θN/θS), (d) number of private alleles, and (e) minor allele in the highest frequency (MAHF) were averaged per site, ordered from low to high latitude. Site abbreviations are defined in Figure 2a.

in N_e around 15 kya and 80 kya, compared with other regions which experienced a decrease in N_e around 7 kya and 45 kya (Figure 7e). Leading-edge sites show site-level differentiation, with KR displaying higher contemporary N_e, KR, and DB having specific N_e over time trends, and BB and DB showing distinct LD decay (Figure S10).

The best-fitting models for both the Leading_edge vs. Core_cluster and Baja_cluster vs. South_cluster comparisons all showed no signs of a population split ("ns" in model name; Figure 7b,c; for a complete list of model names and descriptions see https://github.com/z0on/AFS-analysis-with-moments/blob/master/multimodel_inference/moments_multimodels.xlsx). In the northern lineages, the three top models ranked similarly by median AIC, and all suggest secondary contact (i.e., the reconnection of lineages that previously diverged; "sc" in model name), but differ in the number of epochs (i.e., population size changes) and whether there is isolation with migration ("IM" in model name; Figure 7b). The southern lineages also showed high similarity between the top four models' AIC, which differed in whether they had isolation with migration and the number of epochs (Figure 7c). Due to the highly similar fit between multiple models, we did not estimate parameters for the best-fitting model for either population comparison.

SDMs support a potential southern refugia during the Last Glacial Maximum. All models within the SDMs passed the ROC and TSS thresholds (mean ROC = 0.96, mean TSS = 0.83), and were included in the ensemble (Figure 8). Hindcasts of the species' distributional range show very little change from the present day to the Mid-Holocene (Figure 8). However, the SDMs showed a large range contraction at the LGM, with only the southern edge region having high climatic suitability at this time (Figure 8).

4 | DISCUSSION

Characterizing eco-evolutionary processes associated with climate-driven range expansions is essential to predict the frequency, speed, and success of range shifts under global change (Kubisch et al., 2013; Phillips et al., 2011). Our results on the intertidal owl limpet *Lottia gigantea* suggest that anomalies in ocean currents and temperature associated with El Niño events and other MHWs (Sanford et al., 2019) facilitated a pushed wave expansion, resulting in high genetic diversity and minimal genomic differentiation at the leading edge of its range. Consequently, leading-edge populations may have high adaptive potential due to high standing genetic variation, but may also be at risk of maladaptive gene flow from the species' core with subsequent MHWs. The distinctive genomic composition of trailing-edge populations could be driven by limited gene flow, local selection, and historical climatic stability. Taken together, these patterns show how short-term environmental variation such as changes in ocean current patterns, coupled with long-term climatic change such as temperature stability across climatic oscillations, shape intraspecific genomic variation. These findings provide a critical framework for predicting

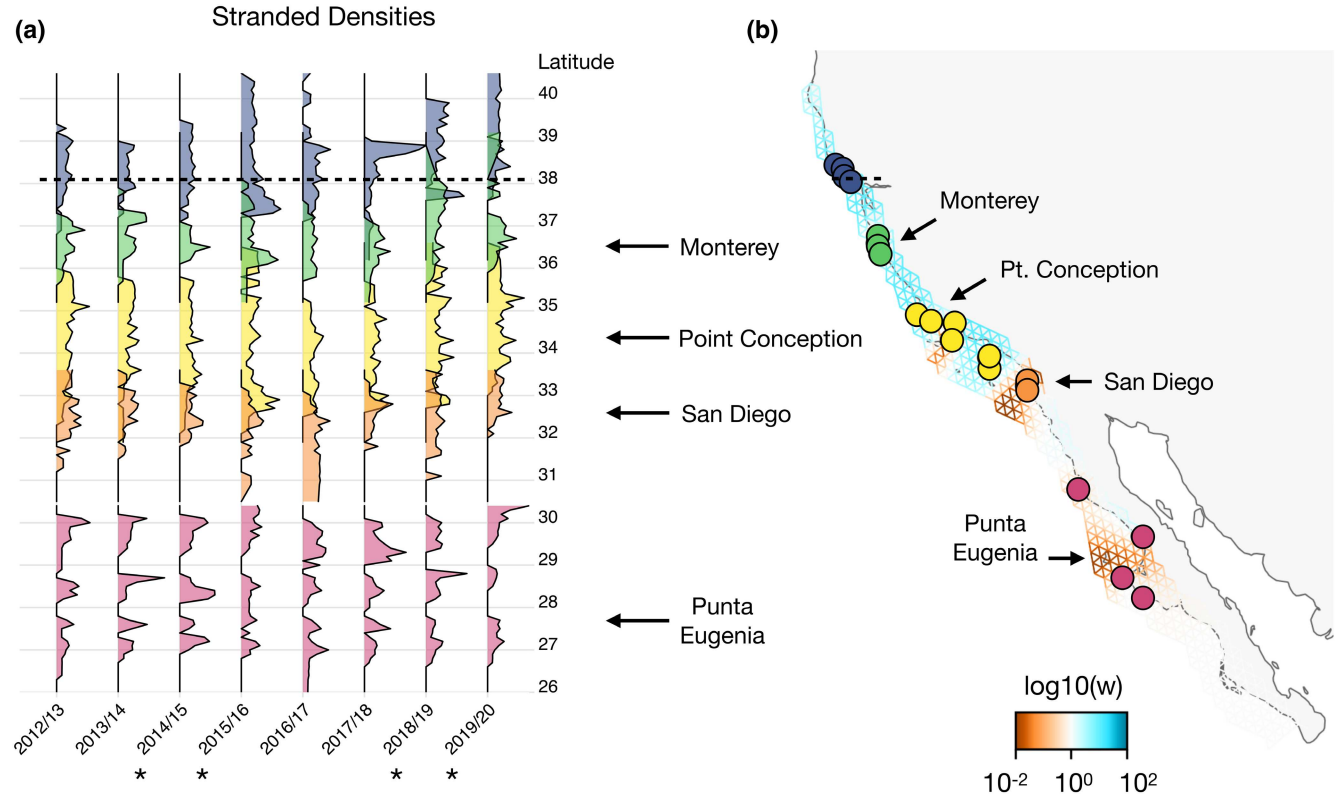

FIGURE 5 Patterns of dispersal and gene flow in *Lottia gigantea*. (a) Estimated density of stranded propagules from larval simulation analyses are shown across latitude for each simulation. Densities are averaged across models run at 12 or 18°C, with higher density representing greater potential for larval recruitment. Years marked with an asterisk indicate those where climatic anomalies are expected to influence recruitment at the expansion front. The dotted line around 38° latitude represents the previous northern range limit for regular recruitment. Colors indicate the source locations where larvae were seeded in the simulations—refer to panel (b) for corresponding colors. (b) A map grid portraying effective migration surfaces, with brown regions indicating lower gene flow than expected given the distance between sites, and blue regions indicating higher than expected gene flow (where *w* is a vector storing elements of the weighted adjacency matrix representing genetic differentiation between subpopulations). Circles indicate sample sites and are colored by the different seeding locations for the larval dispersal simulations.

and interpreting trait evolution across a core-edge gradient in the face of heatwave-driven range expansions.

4.1 | High gene flow within the north, population structuring within the south

Broad-scale phylogeographic structure can help reveal how range expansions and contractions may alter population-level adaptive potential. We found genomic structuring mainly within trailing-edge populations. Consistent with other phylogeographic studies within the region (Bernardi et al., 2003; Eberl et al., 2013; Fenberg et al., 2014; Mares-Mayagoitia et al., 2023; Zarzyczny et al., 2024), our genomic dataset shows two major clusters, with a dominant break near Punta Eugenia, Mexico. Both topography and ocean currents can impede gene flow between marine metapopulations across this break. Specifically, the area around Punta Eugenia is characterized by cyclonic eddies on either side, offshore flow within the southern California current, and a strong temperature transition (Herrera-Cervantes et al., 2014; Zaytsev et al., 2003). We also found a phylogeographic break within the Los Angeles region (LAR, ca. 33.5^0 latitude) and Ensenada Front (ca. 32° latitude), which have been reported in other marine species (Dawson, 2001), such as the isopod *Ligia occidentalis* (Eberl et al., 2013) and the tidewater goby *Eucyclogobius newberryi* (Dawson et al., 2002). This region encompassing LAR and the Ensenada Front is characterized by long stretches of sandy habitat impeding gene flow for rocky shore obligates (Bernardi et al., 2007; Kuo & Sanford, 2013), topographic changes during past climatic oscillations, and the unique seasonal eddies and upwelling of the Ensenada Front where the California Current comes nearshore (Haury et al., 1993).

Within the southern portion of the range, the two San Diego sites and two northern Mexico sites formed a separate cluster ("Baja_cluster"; Figure 3, Figure S4). Earlier work reports similar findings, including high gene flow between populations of the eelgrass *Zostera marina* (Muñiz-Salazar et al., 2005) and the rocky intertidal gastropod *Mexacanthina lugubris* (Fenberg et al., 2014) in the region. The lack of genetic differentiation within the Baja_cluster sites could also be due to El Niños, which create poleward flowing currents within northern Baja California. However, the

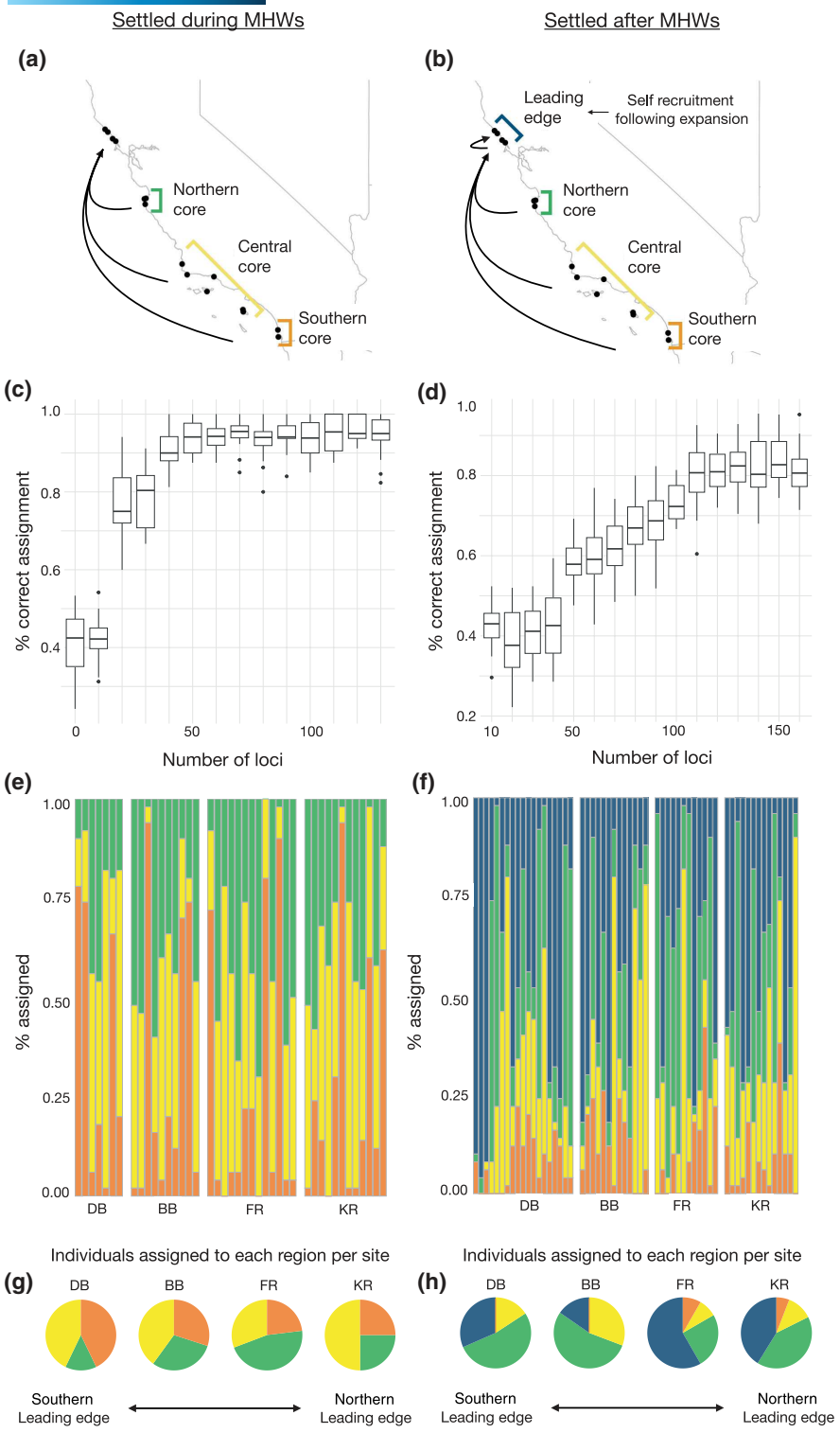

FIGURE 6 Population assignment tests for the four leading-edge sites on individuals that settled during (a); or after the marine heatwaves (MHWs) (b). Sample sites were delineated into different source regions, shown here with arrows indicating potential dispersal (a, b). Mean assignment rates are shown for all single-nucleotide polymorphisms (SNPs) selected from the Guided Regularized Random Forest models (included 10 at a time based on importance scores; c, d). Assignments are shown as the likelihood each individual is from the different source regions (e, f) or as the number of individuals assigned to each source region per site (g, h). Individuals which arrived after the heatwave are plotted left to right per site in ascending order from smallest to largest, as a proxy for the timing of settlement (e, f).

larval simulation models suggest limited larval connectivity between the San Diego and Mexico sites. The discrepancy between larval simulation and genomic differentiation outputs could be due to temporal variation in spawning months across the species range. Preliminary results rearing *L. gigantea* larvae suggest that spawning times differ somewhat between the northern and

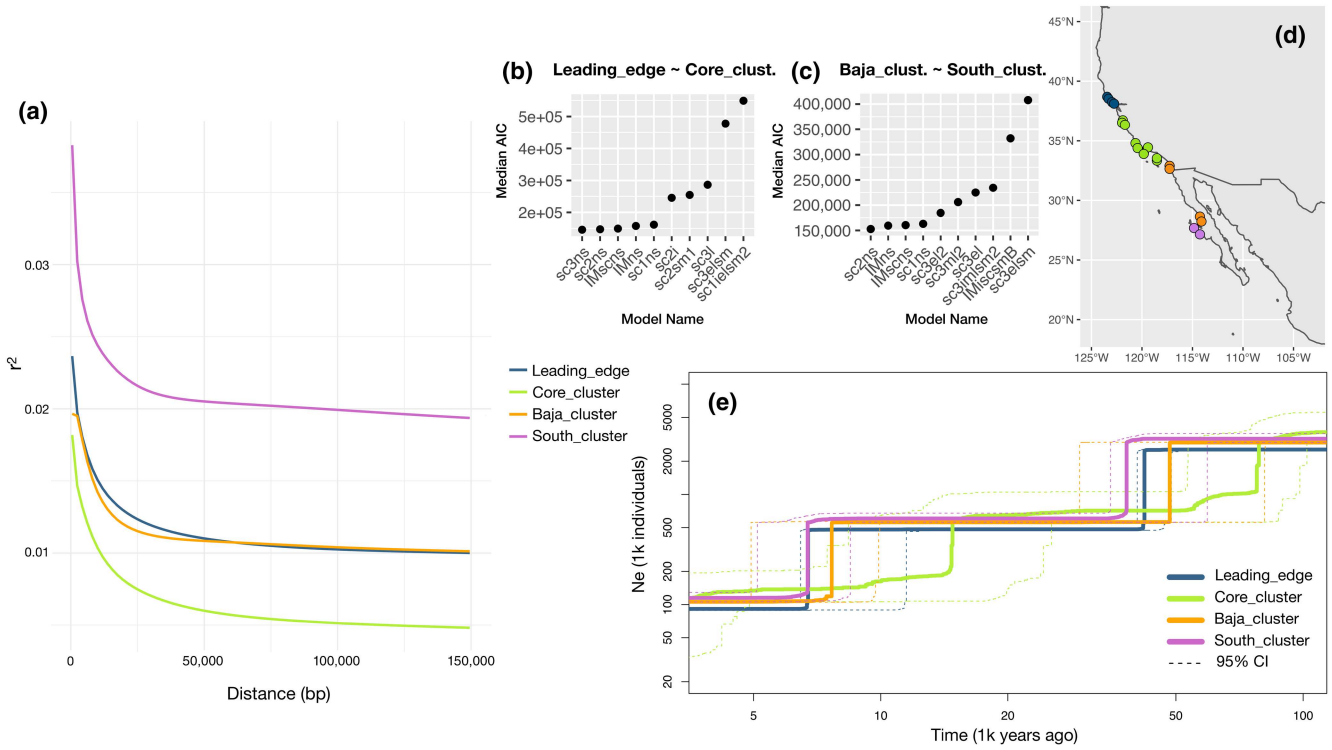

FIGURE 7 Genomic inferences of demographic history for *Lottia gigantea*. (a) Estimates of linkage disequilibrium (LD), represented by the squared correlation (r^2) between two loci, is shown with the best-fit line of decay for each cluster. The top 10 models selected by Moments are shown for comparisons between northern lineages Leading_edge vs. Core_cluster (b) or southern lineages Baja_cluster vs. South_cluster (c), listed by their median AIC scores. Population delineations and corresponding colors are shown (d), along with a stairway plot of each regions' change in effective population size (N_e) through time (e).

central California sites (Sanford et al., unpublished data), and as such, our larval simulation models should be regarded as broad larval dispersal patterns which can be refined in the future. The region between San Diego and Punta Eugenia had slightly higher climatic suitability than the northern part of the range, and lower climatic suitability than the southern Mexico sites during the LGM, and thus, this shared climatic past might also be influencing the genomic distinctiveness of the Baja_cluster.

We did not find genomic structuring across well-known phylogeographic breaks, such as Point Conception and Monterey Bay within the northern part of *L. gigantea* range (Dawson, 2001; Pelc et al., 2009; Wares et al., 2001). The FEEMs analysis was the only one to report a genetic break around Point Conception. That signal was driven by the IP site, which had highly distinct genomic differentiation (shown by the FEEMs output without IP resulting in no break around Point Conception; Figure S11). While this site had the lowest coverage, there were still high levels of differentiation when low coverage individuals were removed (Figure S12). The lack of phylogeographic structure within the northern California region could be related to abundant rocky shore habitat, bi-directional gene flow facilitated by the southern flowing California Current and the northern flowing Davidson Current, nearshore northward flowing currents during *L. gigantea* spawning months, and stochastic events such as upwelling relaxation and El Niños (Fenberg & Rivadeneira, 2011; R. P. Kelly & Palumbi, 2010; Sanford et al., 2019; Wares et al., 2001). The little genomic differentiation over the Central-Northern California (KR-SH sites, Figure 2) and California-Mexico (SC-SR sites; Figure 2) regions and no significant IBD points to the relatively high-dispersal capacity of *L. gigantea*. While the minimum PLD of *L. gigantea* is ca. 4 days, the maximum PLD is 18–21 days (Sanford et al., unpublished data), which potentially allows for larval dispersal over greater distances than what is often considered possible for lecithotrophic species (Weersing & Toonen, 2009).

4.2 | Pushed wave expansion at leading edge

Our results support a pushed wave expansion: the leading edge showed little genomic differentiation from the distributional core, no significant decrease in genomic diversity, low assignment rates from the northern part of the species' range, and no increase in private alleles or minor alleles in highest frequency (Figures 3–5). This pattern contrasts other studies assessing the genomic composition of marine leading-edge populations. For example, the expanded range of the coral *Acropora hyacinthus* had lower genomic diversity, higher LD decay, and was genetically differentiated from the northern core populations (Fifer et al., 2022). Likewise, population structure between the expanded range and core populations was found for the intertidal gastropod, *Nerita yoldii*, along the Chinese coast (Wang et al., 2022) and the octopus *Octopus tetricus*, along

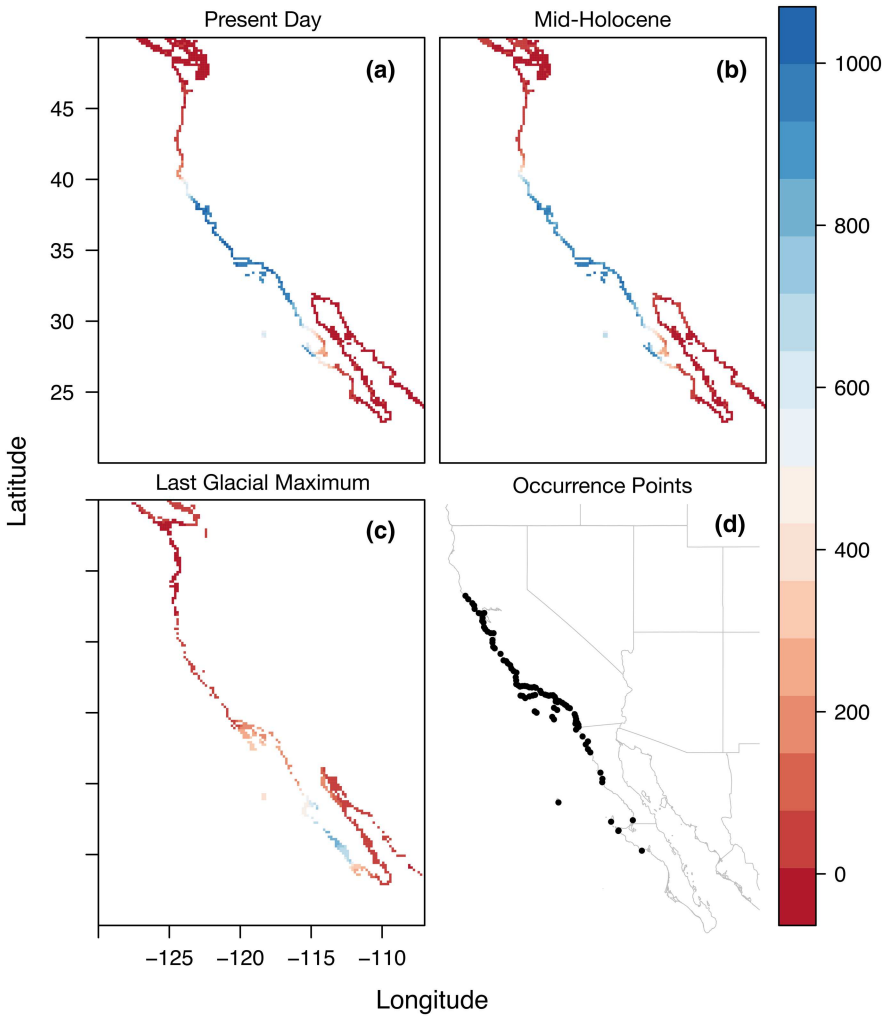

FIGURE 8 Hindcasted distributional shifts for *Lottia gigantea*. Species distribution model climatic suitability maps, with suitability ranging from 0 to 1000, are shown for the present day (a), Mid-Holocene (6 kya; b), and Last Glacial Maximum (21 kya; c). Areas in red represent low climatic suitability (i.e., where the species is likely absent) and areas in blue represent high climatic suitability (i.e., where the species is likely present). Climatic suitability during the Last Glacial Maximum is overlaid onto available coastal habitat with the associated drop in sea level of the period. Input occurrence points are shown in panel (d).

the western Australian coast (Ramos et al., 2018). In contrast, our results mirror those seen in a range expansion of the sea urchin, *Centrostephanus rodgersii* (Banks et al., 2010), the oyster, *Crassostrea sikamea* (Hu & Dong, 2022), and the barnacle, *Tetraclita rubescens* (Dawson et al., 2010), showing no evidence of population structure or a decrease in genetic diversity at the expanded-range edge.

These findings highlight the diverse patterns of genomic variation observed among range expansions in marine systems. Fifer et al. (2022) found the strongest evidence of a pulled wave, with both structure and decreased genetic diversity at the expanding range edge; but others have found less consistent evidence, with genetic differentiation of the expanded range, but not a significant decrease in genetic diversity (Ramos et al., 2018; Wang et al., 2022). These three studies evidencing pulled waves (Fifer et al., 2022; Ramos et al., 2018; Wang et al., 2022) are similar to the examples more consistent with pushed waves (Banks et al., 2010; Dawson et al., 2010; Hu & Dong, 2022) in that they occur in regions experiencing prolonged ocean warming and prevailing ocean currents aligning with the direction of the range expansion. In addition, the species in these examples have high-dispersal potential, with pelagic larval durations ranging from 1 to 4 months. As such, it is unlikely that pulled versus pushed wave expansions are determined by the rate of warming, ocean current direction, or pelagic larval duration.

Of these studies, we can compare species that either show genetic differentiation or not at the expanded-range edge in two regions: southeastern Australia and northeastern China. Both the octopus *O. tetricus* and urchin *C. rodgersii* expanded from the southeastern point of Australia into Tasmania, with the first detections in the expanded range in the early 2000s (Banks et al., 2010; Ramos et al., 2018), demonstrating how patterns of pulled or pushed waves can occur within the same system and timescale. It could be that *C. rodersii* shows no genetic structure at the range edge because it spawns during the summer months, when the East Australian

Current is the strongest, compared with *O. tetricus* which spawns year round. This discrepancy is similar in the two species that expanded along China's coast, with the expanded range of the oyster *C. sikamea* showing lower genetic differentiation compared with the snail *N. yoldii*, which could be driven by the oyster spawning in the summer months when northward currents are strongest. Similarly, *Lottia gigantea* spawns during the winter when poleward currents are the strongest (Sanford et al., 2019). The environmental novelty of the expanded-range habitat could also be an important driver of whether an expansion mirrors pulled or pushed waves. Most of these studies found high amounts of gene flow to the expansion front, but it is those that report discrete environmental pressures such as a new thermal niche in the expanded range, which found genomic variation aligning more with pulled waves (Fifer et al., 2022; Ramos et al., 2018; Wang et al., 2022).

Our study differs from these examples in that the range shift was observed with an extreme climatic event rather than gradual warming. Thus, more genomic inferences of extreme event-driven expansions are needed to gain a holistic picture of the drivers of pulled versus pushed waves. The MHWs were characterized by anomalously strong poleward flows along the central and northern California coast during the fall and winter months when *L. gigantea* larvae are in the water column (Sanford et al., 2019), which could lead to pushed wave dynamics. Our findings suggest that large numbers of individuals can disperse from the species' core to edge during MHWs, which might make extreme events important contributors to pushed waves compared with long-term climatic velocity patterns (Cimino et al., 2021; Miller et al., 2020).

Despite greater overall support of a pushed wave, we find evidence of increased genetic load at the expansion front, with the northern populations harboring higher $\theta N/\theta S$ than the core (which is more indicative of a pulled wave). In the above example that aligns more closely with the pulled wave model, Fifer et al. (2022) found lower levels of genetic load within the northern edge populations, which they attribute to environmental selection driving high levels of purifying selection. As the stairway analysis suggests that the contemporary leading-edge populations have lower N_e compared with the rest of the range, it could be that small population sizes are driving higher LD and genomic load within the leading edge (i.e., due to genetic drift rather than selection). By assessing multiple genomic metrics, such as genetic load, gene flow, diversity, and allele surfing, we can better tease apart the eco-evolutionary feedbacks occurring during range expansions, which are likely more nuanced than pulled versus pushed wave dynamics. This study also offers an exciting first step in understanding eco-evolutionary dynamics over time, as subsequent sampling can help elucidate how range expansions may shift from pushed to pulled waves (Erm & Phillips, 2020). For example, if population growth following the initial event relies heavily on self-recruitment, genomic and phenotypic variabily will likely change from pushed to pulled wave characteristics.

4.3 | Unique evolutionary composition of trailing-edge populations

Trailing edges remain largely understudied compared with their leading-edge counterparts (Thuiller et al., 2008), and few studies assess evolutionary processes across both trailing and leading edges (Hampe & Petit, 2005). We find that the southern edge of the species' range shows a distinct evolutionary trajectory, with high levels of population differentiation, increased genomic diversity and unique alleles, and low levels of gene flow. Previous work on *L. gigantea* suggests that the southern portion of the species' range has higher amounts of habitat fragmentation owing to long stretches of sandy shore (Fenberg & Rivadeneira, 2011), which could impede recruitment and gene flow. This habitat fragmentation and low gene flow, in combination with Allee effects, could create an eco-evolutionary feedback furthering differentiation of the southern populations (Maciel & Lutscher, 2015). The southern edge also experiences different environmental conditions than the rest of the species' range, with higher sea surface, air, and rock temperatures, lower oxygen levels, and the lack of biogenic habitats to facilitate recruitment such as mussel beds and giant kelp (Bernardi et al., 2003; Lohse, 1993; Pondella II et al., 2005), indicating that local selection could further lead to genomic differentiation among these sites (O'Connor et al., 2007).

Several studies suggest that past climatic-driven range dynamics are stronger predictors of genetic diversity than contemporary demographic patterns, and can lead to marginal populations being highly diverse (Chefaoui & Serrão, 2017; Hewitt, 2004; Petit, 2003; Zarzyczny et al., 2024). We found that the southern edge of the range had higher climatic suitability at the LGM, which suggests that this region could have high genetic diversity due to it being a climatically stable refugium (Beatty & Provan, 2011; Hellberg et al., 2001; Waltari & Hickerson, 2013; Zarzyczny et al., 2024). The Moments demographic analyses suggest that Baja_cluster and South_cluster have a shared demographic history and thus were similarly impacted by the changes since the LGM. However, the stairway plot suggests that the South_cluster had slightly different changes in N_e over time. These populations likely experienced changes in ocean currents and topography distinctly (as shown by their distinct larval simulation and genomic patterns), yet had enough intermittent gene flow that they remained a single lineage through time.

Our findings point to the southern edge as an evolutionary distinct unit, which corroborates work suggesting that trailing-edge populations are of conservation concern due to their unique genetic composition (Budd & Pandolfi, 2010; Cocito et al., 2019; Rodríguez-Muñoz et al., 2007; Saada et al., 2016). These relict peripheral populations may be important sources of warm-adapted individuals as ocean warming continues to intensify (Kelly, 2019), but given that we found a lack of gene flow from the southern Mexico sites, assisted migration may be needed to supplement core populations. A better understanding of trailing-edge demographics is needed, as Allee effects have been shown to be particularly important in the pace of

range contractions, with areas of low fitness at low densities being at higher risk of local extinctions (Kubisch et al., 2013). As *L. gigantea* is undergoing a range contraction near the southern edge of its range (Fenberg et al., unpublished data), this evolutionarily distinct unit is at greater risk of local extirpation, and conservation intervention might be warranted.

5 | CONCLUSIONS

This work emphasizes that range edge populations can have distinct evolutionary dynamics, even within species with relatively high gene flow and dispersal capacity (compared with other gastropods; Kelly & Palumbi, 2010). Moreover, we show how extreme climatic events may be important drivers of pushed wave expansions, which has important eco-evolutionary implications with regard to expansion rates and adaptive potential of the range edge. As we begin to understand ecological and evolutionary feedbacks during range expansions, it is essential that both long-term and acute climatic velocities are considered (Chapman et al., 2014), especially as extreme events such as MHWs are increasing in frequency and intensity (Oliver et al., 2018). This holistic approach will allow for more accurate predictions of whether leading-edge populations will be able to keep pace with extirpations at the trailing edge, and if trailing and leading edges will require distinct conservation efforts under global change (Thompson et al., 2023).

AUTHOR CONTRIBUTIONS

Erica S. Nielsen: Data curation; formal analysis; investigation; methodology; project administration; visualization; writing – original draft; writing – review and editing. **Samuel Walkes:** Data curation; investigation; writing – review and editing. **Jacqueline L. Sones:** Conceptualization; data curation; investigation; resources; validation; writing – review and editing. **Phillip B. Fenberg:** Data curation; writing – review and editing. **David A. Paz-García:** Data curation; writing – review and editing. **Brenda B. Cameron:** Data curation; resources; writing – review and editing. **Richard K. Grosberg:** Conceptualization; funding acquisition; investigation; supervision; validation; writing – review and editing. **Eric Sanford:** Conceptualization; data curation; funding acquisition; investigation; resources; supervision; validation; writing – review and editing. **Rachael A. Bay:** Conceptualization; funding acquisition; investigation; methodology; project administration; resources; supervision; validation; writing – review and editing.

ACKNOWLEDGEMENTS

We thank Camille Rumberger, Laura Dennis, and Andrea Puga for field assistance. We also thank Nicole Adams, Knut-Frode Dagestad, Craig Norrie, TJ Olesky, and Aryn Wilder for their assistance with code/bioinformatics. Much of the bioinformatics was based on publicly available code by Claire Mérot. This research was funded by NSF grant OCE-2023297 and supplement OCE-2322845. We are grateful to the UC Natural Reserve System, California State Parks, Cabrillo National Monument, Channel Islands National Park, Hopkins Marine Station, Greater Farallones and Monterey Bay National Marine Sanctuaries, The Nature Conservancy, and Vandenberg Space Force Base for access to field sites. The permit to collect the samples in Mexico was provided by the Secretaría de Agricultura, Ganadería, Desarrollo Rural, Pesca y Alimentación (SAGARPA, Permiso de Pesca de Fomento No. PPF/DGOPA-291/17 and PPF/DGOPA-010/19). We thank the anonymous reviewers for their comments and suggestions.

CONFLICT OF INTEREST STATEMENT

The authors declare no conflicts of interest.

DATA AVAILABILITY STATEMENT

Raw genomic read data can be found on the sequence read archive under SRA BioProject accession number: PRJNA1075458. The data and scripts that support the findings of this study are openly available inthe Github repository at https://github.com/esnielsen/Lottia_range_expansion/tree/main and Zenodo at with DOI: https://doi.org/10.5281/zenodo.10723308. .

ORCID

Erica S. Nielsen https://orcid.org/0000-0002-5439-571X
Phillip B. Fenberg https://orcid.org/0000-0002-0167-6788
David A. Paz-García https://orcid.org/0000-0002-1228-5221
Richard K. Grosberg https://orcid.org/0000-0003-4162-1375
Eric Sanford https://orcid.org/0000-0002-9232-9334
Rachael A. Bay https://orcid.org/0000-0002-9516-5881

REFERENCES

Andrade-Restrepo, M., Champagnat, N., & Ferrière, R. (2019). Local adaptation, dispersal evolution, and the spatial eco-evolutionary dynamics of invasion. *Ecology Letters*, *22*(5), 767–777. https://doi.org/10.1111/ele.13234

Banks, S. C., Ling, S. D., Johnson, C. R., Piggott, M. P., Williamson, J. E., & Beheregaray, L. B. (2010). Genetic structure of a recent climate change-driven range extension. *Molecular Ecology*, *19*(10), 2011–2024. https://doi.org/10.1111/j.1365-294X.2010.04627.x

Bates, A. E., Pecl, G. T., Frusher, S., Hobday, A. J., Wernberg, T., Smale, D. A., Sunday, J. M., Hill, N. A., Dulvy, N. K., Colwell, R. K., Holbrook, N. J., Fulton, E. A., Slawinski, D., Feng, M., Edgar, G. J., Radford, B. T., Thompson, P. A., & Watson, R. A. (2014). Defining and observing stages of climate-mediated range shifts in marine systems. *Global Environmental Change*, *26*, 27–38. https://doi.org/10.1016/j.gloenvcha.2014.03.009

Beatty, G. E., & Provan, J. (2011). Phylogeographic analysis of north American populations of the parasitic herbaceous plant *Monotropa hypopitys* L. reveals a complex history of range expansion from multiple late glacial refugia. *Journal of Biogeography*, *38*(8), 1585–1599. https://doi.org/10.1111/j.1365-2699.2011.02513.x

Bernardi, G., Findley, L., & Rocha-Olivares, A. (2003). Vicariance and dispersal across Baja California in disjunct marine fish populations. *Evolution*, *57*(7), 1599–1609. https://doi.org/10.1111/j.0014-3820.2003.tb00367.x

Bernardi, G., Ruiz-Campos, G., & Camarena-Rosales, F. (2007). Genetic isolation and evolutionary history of oases populations of the Baja California killifish. *Fundulus Lima Conservation Genetics*, *8*(3), 547–554. https://doi.org/10.1007/s10592-006-9190-1

Bestion, E., Clobert, J., & Cote, J. (2015). Dispersal response to climate change: Scaling down to intraspecific variation. *Ecology Letters*, *18*(11), 1226–1233. https://doi.org/10.1111/ele.12502

Blanchette, C. A., Melissa Miner, C., Raimondi, P. T., Lohse, D., Heady, K. E. K., & Broitman, B. R. (2008). Biogeographical patterns of rocky intertidal communities along the Pacific coast of North America. *Journal of Biogeography*, *35*(9), 1593–1607. https://doi.org/10.1111/j.1365-2699.2008.01913.x

Bonnefon, O., Coville, J., Garnier, J., Hamel, F., & Roques, L. (2014). The spatio-temporal dynamics of neutral genetic diversity. *Ecological Complexity*, *20*, 282–292. https://doi.org/10.1016/j.ecocom.2014.05.003

Breese, M. R., & Liu, Y. (2013). NGSUtils: A software suite for analyzing and manipulating next-generation sequencing datasets. *Bioinformatics*, *29*(4), 494–496. https://doi.org/10.1093/bioinformatics/bts731

Budd, A. F., & Pandolfi, J. M. (2010). Evolutionary novelty is concentrated at the edge of coral species distributions. *Science*, *328*(5985), 1558–1561. https://doi.org/10.1126/science.1188947

Burford, B. P., Wild, L. A., Schwarz, R., Chenoweth, E. M., Sreenivasan, A., Elahi, R., Carey, N., Hoving, H.-J. T., Straley, J. M., & Denny, M. W. (2022). Rapid range expansion of a marine ectotherm reveals the demographic and ecological consequences of short-term variability in seawater temperature and dissolved oxygen. *The American Naturalist*, *199*(4), 523–550. https://doi.org/10.1086/718575

Burrows, M. T., Schoeman, D. S., Buckley, L. B., Moore, P., Poloczanska, E. S., Brander, K. M., Brown, C., Bruno, J. F., Duarte, C. M., Halpern, B. S., Holding, J., Kappel, C. V., Kiessling, W., O'Connor, M. I., Pandolfi, J. M., Parmesan, C., Schwing, F. B., Sydeman, W. J., & Richardson, A. J. (2011). The pace of shifting climate in marine and terrestrial ecosystems. *Science*, *334*(6056), 652–655. https://doi.org/10.1126/science.1210288

Chapman, S., Mustin, K., Renwick, A. R., Segan, D. B., Hole, D. G., Pearson, R. G., & Watson, J. E. M. (2014). Publishing trends on climate change vulnerability in the conservation literature reveal a predominant focus on direct impacts and long time-scales. *Diversity and Distributions*, *20*(10), 1221–1228. https://doi.org/10.1111/ddi.12234

Chefaoui, R. M., & Serrão, E. A. (2017). Accounting for uncertainty in predictions of a marine species: Integrating population genetics to verify past distributions. *Ecological Modelling*, *359*, 229–239. https://doi.org/10.1016/j.ecolmodel.2017.06.006

Chen, S., Zhou, Y., Chen, Y., & Gu, J. (2018). Fastp: An ultra-fast all-in-one FASTQ preprocessor. *Bioinformatics*, *34*(17), i884–i890. https://doi.org/10.1093/bioinformatics/bty560

Chen, Z., Doğan, Ö., Guiglielmoni, N., Guichard, A., & Schrödl, M. (2022). Pulmonate slug evolution is reflected in the de novo genome of *Arion vulgaris* Moquin-Tandon, 1855. *Scientific Reports*, *12*(1), 14226. https://doi.org/10.1038/s41598-022-18099-7

Cimino, M. A., Jacox, M. G., Bograd, S. J., Brodie, S., Carroll, G., Hazen, E. L., Lavaniegos, B. E., Morales, M. M., Satterthwaite, E., & Rykaczewski, R. R. (2021). Anomalous poleward advection facilitates episodic range expansions of pelagic red crabs in the eastern North Pacific. *Limnology and Oceanography*, *66*(8), 3176–3189. https://doi.org/10.1002/lno.11870

Cocito, L. L., Ceballos, S. G., & Fernández, D. A. (2019). Sharp phylogeographical differentiation near the southern range edge of the silverside *Odontesthes nigricans*: Distinct peripheral populations and incipient speciation? *Estuarine, Coastal and Shelf Science*, *226*, 106276. https://doi.org/10.1016/j.ecss.2019.106276

Coleman, M. A., Minne, A. J. P., Vranken, S., & Wernberg, T. (2020). Genetic tropicalisation following a marine heatwave. *Scientific Reports*, *10*(1), 12726. https://doi.org/10.1038/s41598-020-69665-w

Dagestad, K.-F., Röhrs, J., Breivik, Ø., & Ådlandsvik, B. (2017). OpenDrift v1.0: A generic framework for trajectory modeling. *Geoscientific Model Development*, *11*(4), 1405–1420. https://doi.org/10.5194/gmd-2017-205

Daly, G. P. (1975). *Growth and reproduction in the marine limpet Lottia gigantea (gray) (Acmaeidae)*. MSc Thesis. San Diego State University.

Dawson, M. N. (2001). Phylogeography in coastal marine animals: A solution from California? *Journal of Biogeography*, *28*(6), 723–736. https://doi.org/10.1046/j.1365-2699.2001.00572.x

Dawson, M. N., Grosberg, R. K., Stuart, Y. E., & Sanford, E. (2010). Population genetic analysis of a recent range expansion: Mechanisms regulating the poleward range limit in the volcano barnacle *Tetraclita rubescens*. *Molecular Ecology*, *19*(8), 1585–1605. https://doi.org/10.1111/j.1365-294X.2010.04588.x

Dawson, M. N., Louie, K. D., Barlow, M., Jacobs, D. K., & Swift, C. C. (2002). Comparative phylogeography of sympatric sister species, *Clevelandia ios* and *Eucyclogobius newberryi* (Teleostei, Gobiidae), across the California transition zone. *Molecular Ecology*, *11*(6), 1065–1075. https://doi.org/10.1046/j.1365-294X.2002.01503.x

Deng, H., & Runger, G. (2013). Gene selection with guided regularized random forest. *Pattern Recognition*, *46*(12), 3483–3489. https://doi.org/10.1016/j.patcog.2013.05.018

Eberl, R., Mateos, M., Grosberg, R. K., Santamaria, C. A., & Hurtado, L. A. (2013). Phylogeography of the supralittoral isopod *Ligia occidentalis* around the point conception marine biogeographical boundary. *Journal of Biogeography*, *40*(12), 2361–2372. https://doi.org/10.1111/jbi.12168

Erm, P., & Phillips, B. L. (2020). Evolution transforms pushed waves into pulled waves. *The American Naturalist*, *195*(3), E87–E99.

Fenberg, P. B., Hellberg, M. E., Mullen, L., & Roy, K. (2010). Genetic diversity and population structure of the size-selectively harvested owl limpet, *Lottia gigantea*: Genetic diversity and population structure. *Marine Ecology*, *31*(4), 574–583. https://doi.org/10.1111/j.1439-0485.2010.00386.x

Fenberg, P. B., Posbic, K., & Hellberg, M. E. (2014). Historical and recent processes shaping the geographic range of a rocky intertidal gastropod: Phylogeography, ecology, and habitat availability. *Ecology and Evolution*, *4*(16), 3244–3255. https://doi.org/10.1002/ece3.1181

Fenberg, P. B., & Rivadeneira, M. M. (2011). Range limits and geographic patterns of abundance of the rocky intertidal owl limpet, *Lottia gigantea*: Range limits and geographic patterns of abundance. *Journal of Biogeography*, *38*(12), 2286–2298. https://doi.org/10.1111/j.1365-2699.2011.02572.x

Fenberg, P. B., & Roy, K. (2012). Anthropogenic harvesting pressure and changes in life history: Insights from a rocky intertidal limpet. *The American Naturalist*, *180*(2), 200–210. https://doi.org/10.1086/666613

Fewings, M. R., & Brown, K. S. (2019). Regional structure in the marine heat wave of summer 2015 off the western United States. *Frontiers in Marine Science*, *6*, 564. https://doi.org/10.3389/fmars.2019.00564

Fifer, J. E., Yasuda, N., Yamakita, T., Bove, C. B., & Davies, S. W. (2022). Genetic divergence and range expansion in a western North Pacific coral. *Science of the Total Environment*, *813*, 152423. https://doi.org/10.1016/j.scitotenv.2021.152423

García Molinos, J., Hunt, H. L., Green, M. E., Champion, C., Hartog, J. R., & Pecl, G. T. (2022). Climate, currents and species traits contribute to early stages of marine species redistribution. *Communications Biology*, *5*(1), 1329. https://doi.org/10.1038/s42003-022-04273-0

Garnier, J., & Lewis, M. A. (2016). Expansion under climate change: The genetic consequences. *Bulletin of Mathematical Biology*, *78*(11), 2165–2185. https://doi.org/10.1007/s11538-016-0213-x

Gautier, M. (2015). *BAYPASS version 2.1 user manual.*

Goslee, S. C., & Urban, D. L. (2007). The ecodist package for dissimilarity-based analysis of ecological data. *Journal of Statistical Software*, *22*(7), 1–19. https://doi.org/10.18637/jss.v022.i07

Hallatschek, O., & Nelson, D. R. (2008). Gene surfing in expanding populations. *Theoretical Population Biology*, *73*(1), 158–170. https://doi.org/10.1016/j.tpb.2007.08.008

Hampe, A., & Petit, R. J. (2005). Conserving biodiversity under climate change: The rear edge matters: Rear edges and climate change. *Ecology Letters*, *8*(5), 461–467. https://doi.org/10.1111/j.1461-0248.2005.00739.x

Hardie, D. C., & Hutchings, J. A. (2010). Evolutionary ecology at the extremes of species' ranges. *Environmental Reviews*, *18*, 1–20. https://doi.org/10.1139/A09-014

Harvey, B. P., Marshall, K. E., Harley, C. D. G., & Russell, B. D. (2022). Predicting responses to marine heatwaves using functional traits. *Trends in Ecology & Evolution*, *37*(1), 20–29. https://doi.org/10.1016/j.tree.2021.09.003

Hastings, R. A., Rutterford, L. A., Freer, J. J., Collins, R. A., Simpson, S. D., & Genner, M. J. (2020). Climate change drives poleward increases and equatorward declines in marine species. *Current Biology*, *30*(8), 1572–1577.e2. https://doi.org/10.1016/j.cub.2020.02.043

Haury, L. R., Venrick, E. L., Fey, C. L., McGowan, J. A., & Niiler, P. P. (1993). *The Ensenada Front: July 1985. CalCOFI Report*. Vol. 34.

Hellberg, M. E., Balch, D. P., & Roy, K. (2001). Climate-driven range expansion and morphological evolution in a marine gastropod. *Science*, *292*(5522), 1707–1710. https://doi.org/10.1126/science.1060102

Hemstrom, W., & Jones, M. (2023). snpR: User friendly population genomics for SNP data sets with categorical metadata. *Molecular Ecology Resources*, *23*(4), 962–973. https://doi.org/10.1111/1755-0998.13721

Henry, R. C., Bocedi, G., & Travis, J. M. J. (2013). Eco-evolutionary dynamics of range shifts: Elastic margins and critical thresholds. *Journal of Theoretical Biology*, *321*, 1–7. https://doi.org/10.1016/j.jtbi.2012.12.004

Herrera-Cervantes, H., Lluch-Cota, S. E., Lluch-Cota, D. B., & Gutiérrez-de-Velasco, G. (2014). Interannual correlations between sea surface temperature and concentration of chlorophyll pigment off Punta Eugenia, Baja California, during different remote forcing conditions. *Ocean Science*, *10*(3), 345–355. https://doi.org/10.5194/os-10-345-2014

Hewitt, G. M. (2004). Genetic consequences of climatic oscillations in the quaternary. *Philosophical Transactions of the Royal Society of London. Series B: Biological Sciences*, *359*(1442), 183–195. https://doi.org/10.1098/rstb.2003.1388

Hu, L., & Dong, Y. (2022). Multiple genetic sources facilitate the northward range expansion of an intertidal oyster along China's coast. *Ecological Applications*, *34*(1), e2764. https://doi.org/10.1002/eap.2764

Jouganous, J., Long, W., Ragsdale, A. P., & Gravel, S. (2017). Inferring the joint demographic history of multiple populations: Beyond the diffusion approximation. *Genetics*, *206*(3), 1549–1567. https://doi.org/10.1534/genetics.117.200493

Kelly, M. (2019). Adaptation to climate change through genetic accommodation and assimilation of plastic phenotypes. *Philosophical Transactions of the Royal Society, B: Biological Sciences*, *374*(1768), 20180176. https://doi.org/10.1098/rstb.2018.0176

Kelly, R. P., & Palumbi, S. R. (2010). Genetic structure among 50 species of the northeastern Pacific rocky intertidal community. *PLoS One*, *5*(1), e8594. https://doi.org/10.1371/journal.pone.0008594

Kerr, J. T. (2020). Racing against change: Understanding dispersal and persistence to improve species' conservation prospects. *Proceedings of the Royal Society B: Biological Sciences*, *287*(1939), 20202061. https://doi.org/10.1098/rspb.2020.2061

Kido, J., & Murray, S. (2003). Variation in owl limpet *Lottia gigantea* population structures, growth rates, and gonadal production on southern California rocky shores. *Marine Ecology Progress Series*, *257*, 111–124. https://doi.org/10.3354/meps257111

Korneliussen, T. S., Albrechtsen, A., & Nielsen, R. (2014). ANGSD: Analysis of next generation sequencing data. *BMC Bioinformatics*, *15*(1), 356. https://doi.org/10.1186/s12859-014-0356-4

Korunes, K. L., & Samuk, K. (2021). Pixy: Unbiased estimation of nucleotide diversity and divergence in the presence of missing data. *Molecular Ecology Resources*, *21*(4), 1359–1368. https://doi.org/10.1111/1755-0998.13326

Kubisch, A., Degen, T., Hovestadt, T., & Poethke, H. J. (2013). Predicting range shifts under global change: The balance between local adaptation and dispersal. *Ecography*, *36*(8), 873–882. https://doi.org/10.1111/j.1600-0587.2012.00062.x

Kuo, E. S. L., & Sanford, E. (2013). Northern distribution of the seaweed limpet *Lottia insessa* (Mollusca: Gastropoda) along the Pacific Coast1. *Pacific Science*, *67*(2), 303–313. https://doi.org/10.2984/67.2.12

Legrand, D., Cote, J., Fronhofer, E. A., Holt, R. D., Ronce, O., Schtickzelle, N., Travis, J. M. J., & Clobert, J. (2017). Eco-evolutionary dynamics in fragmented landscapes. *Ecography*, *40*(1), 9–25. https://doi.org/10.1111/ecog.02537

Li, H. (2013). *Aligning sequence reads, clone sequences and assembly contigs with BWA-MEM. arXiv:1303.3997 [q-Bio]*. http://arxiv.org/abs/1303.3997

Li, H., Handsaker, B., Wysoker, A., Fennell, T., Ruan, J., Homer, N., Marth, G., Abecasis, G., Durbin, R., & 1000 Genome Project Data Processing Subgroup. (2009). The sequence alignment/map format and SAMtools. *Bioinformatics*, *25*(16), 2078–2079. https://doi.org/10.1093/bioinformatics/btp352

Li, Y., Ren, G., You, Q., Wang, Q., Niu, Q., & Mu, L. (2022). The 2016 record-breaking marine heatwave in the Yellow Sea and associated atmospheric circulation anomalies. *Atmospheric Research*, *268*, 106011. https://doi.org/10.1016/j.atmosres.2021.106011

Lindberg, D. R., Estes, J. A., & Warheit, K. I. (1998). Human influences on trophic cascades along rocky shores. *Ecological Applications*, *8*(3), 880–890. https://doi.org/10.1890/1051-0761(1998)008[0880:HIOTCA]2.0.CO;2

Liu, X., & Fu, Y.-X. (2020). Stairway plot 2: Demographic history inference with folded SNP frequency spectra. *Genome Biology*, *21*(1), 280. https://doi.org/10.1186/s13059-020-02196-9

Lohse, D. P. (1993). The importance of secondary substratum in a rocky intertidal community. *Journal of Experimental Marine Biology and Ecology*, *166*(1), 1–17. https://doi.org/10.1016/0022-0981(93)90075-Y

Lonhart, S. I., Jeppesen, R., Beas-Luna, R., Crooks, J. A., & Lorda, J. (2019). Shifts in the distribution and abundance of coastal marine species along the eastern Pacific Ocean during marine heatwaves from 2013 to 2018. *Marine Biodiversity Records*, *12*(1), 13. https://doi.org/10.1186/s41200-019-0171-8

Maciel, G. A., & Lutscher, F. (2015). Allee effects and population spread in patchy landscapes. *Journal of Biological Dynamics*, *9*(1), 109–123. https://doi.org/10.1080/17513758.2015.1027309

Marcus, J., Ha, W., Barber, R. F., & Novembre, J. (2021). Fast and flexible estimation of effective migration surfaces. *eLife*, *10*, e61927. https://doi.org/10.7554/eLife.61927

Mares-Mayagoitia, J. A., Lafarga-De la Cruz, F., Micheli, F., Cruz-Hernández, P., de-Anda-Montañez, J. A., Hyde, J., Hernández-Saavedra, N. Y., Mejía-Ruíz, P., De Jesús-Bonilla, V. S., Vargas-Peralta, C. E., & Valenzuela-Quiñonez, F. (2023). Seascape genomics of the pink abalone (*Haliotis corrugata*): An insight into a cross-border species in the northeast Pacific coast. *Journal of Heredity*, *115*(2), esad083. https://doi.org/10.1093/jhered/esad083

Marzonie, M. R., Bay, L. K., Bourne, D. G., Hoey, A. S., Matthews, S., Nielsen, J. J. V., & Harrison, H. B. (2023). The effects of marine heatwaves on acute heat tolerance in corals. *Global Change Biology*, *29*(2), 404–416. https://doi.org/10.1111/gcb.16473

McKenna, A., Hanna, M., Banks, E., Sivachenko, A., Cibulskis, K., Kernytsky, A., Garimella, K., Altshuler, D., Gabriel, S., Daly, M., & DePristo, M. A. (2010). The genome analysis toolkit: A MapReduce framework for analyzing next-generation DNA sequencing data. *Genome Research*, *20*(9), 1297–1303. https://doi.org/10.1101/gr.107524.110

McLaren, W., Gil, L., Hunt, S. E., Riat, H. S., Ritchie, G. R. S., Thormann, A., Flicek, P., & Cunningham, F. (2016). The Ensembl variant effect predictor. *Genome Biology*, *17*(1), 122. https://doi.org/10.1186/s13059-016-0974-4

Meisner, J., Albrechtsen, A., & Hanghøj, K. (2021). Detecting selection in low-coverage high-throughput sequencing data using principal component analysis. *BMC Bioinformatics*, *22*(1), 470. https://doi.org/10.1186/s12859-021-04375-2

Miller, T. E. X., Angert, A. L., Brown, C. D., Lee-Yaw, J. A., Lewis, M., Lutscher, F., Marculis, N. G., Melbourne, B. A., Shaw, A. K., Szűcs, M., Tabares, O., Usui, T., Weiss-Lehman, C., & Williams, J. L. (2020). Eco-evolutionary dynamics of range expansion. *Ecology*, *101*(10), e03139. https://doi.org/10.1002/ecy.3139

Muñiz-Salazar, R., Talbot, S. L., Sage, G. K., Ward, D. H., & Cabello-Pasini, A. (2005). Population genetic structure of annual and perennial populations of *Zostera marina* L. along the Pacific coast of Baja California and the Gulf of California. *Molecular Ecology*, *14*(3), 711–722. https://doi.org/10.1111/j.1365-294X.2005.02454.x

Nei, M. (1987). *Molecular evolutionary genetics*. Columbia University Press.

Norberg, J., Urban, M. C., Vellend, M., Klausmeier, C. A., & Loeuille, N. (2012). Eco-evolutionary responses of biodiversity to climate change. *Nature. Climate Change*, *2*(10), 747–751. https://doi.org/10.1038/nclimate1588

O'Connor, M. I., Bruno, J. F., Gaines, S. D., Halpern, B. S., Lester, S. E., Kinlan, B. P., & Weiss, J. M. (2007). Temperature control of larval dispersal and the implications for marine ecology, evolution, and conservation. *Proceedings of the National Academy of Sciences*, *104*(4), 1266–1271. https://doi.org/10.1073/pnas.0603422104

Oliver, E. C. J., Donat, M. G., Burrows, M. T., Moore, P. J., Smale, D. A., Alexander, L. V., Benthuysen, J. A., Feng, M., Sen Gupta, A., Hobday, A. J., Holbrook, N. J., Perkins-Kirkpatrick, S. E., Scannell, H. A., Straub, S. C., & Wernberg, T. (2018). Longer and more frequent marine heatwaves over the past century. *Nature Communications*, *9*(1), 1–12. https://doi.org/10.1038/s41467-018-03732-9

Pelc, R. A., Warner, R. R., & Gaines, S. D. (2009). Geographical patterns of genetic structure in marine species with contrasting life histories. *Journal of Biogeography*, *36*(10), 1881–1890. https://doi.org/10.1111/j.1365-2699.2009.02138.x

Petit, R. J. (2003). Glacial refugia: Hotspots but not melting pots of genetic diversity. *Science*, *300*(5625), 1563–1565. https://doi.org/10.1126/science.1083264

Petkova, D., Novembre, J., & Stephens, M. (2016). Visualizing spatial population structure with estimated effective migration surfaces. *Nature Genetics*, *48*(1), 94–100. https://doi.org/10.1038/ng.3464

Phillips, N. M., Chaplin, J. A., Morgan, D. L., & Peverell, S. C. (2011). Population genetic structure and genetic diversity of three critically endangered *Pristis* sawfishes in Australian waters. *Marine Biology*, *158*(4), 903–915. https://doi.org/10.1007/s00227-010-1617-z

Pinsky, M. L., Selden, R. L., & Kitchel, Z. J. (2020). Climate-driven shifts in marine species ranges: Scaling from organisms to communities. *Annual Review of Marine Science*, *12*(1), 153–179. https://doi.org/10.1146/annurev-marine-010419-010916

Poloczanska, E. S., Brown, C. J., Sydeman, W. J., Kiessling, W., Schoeman, D. S., Moore, P. J., Brander, K., Bruno, J. F., Buckley, L. B., Burrows, M. T., Duarte, C. M., Halpern, B. S., Holding, J., Kappel, C. V., O'Connor, M. I., Pandolfi, J. M., Parmesan, C., Schwing, F., Thompson, S. A., & Richardson, A. J. (2013). Global imprint of climate change on marine life. *Nature Climate Change*, *3*(10), 919–925. https://doi.org/10.1038/nclimate1958

Pondella, D. J., II, Gintert, B. E., Cobb, J. R., & Allen, L. G. (2005). Biogeography of the nearshore rocky-reef fishes at the southern and Baja California islands. *Journal of Biogeography*, *32*(2), 187–201. https://doi.org/10.1111/j.1365-2699.2004.01180.x

Ramos, J. E., Pecl, G. T., Moltschaniwskyj, N. A., Semmens, J. M., Souza, C. A., & Strugnell, J. M. (2018). Population genetic signatures of a climate change driven marine range extension. *Scientific Reports*, *8*(1), 1–12. https://doi.org/10.1038/s41598-018-27351-y

Rodríguez-Muñoz, R., Mirol, P. M., Segelbacher, G., Fernández, A., & Tregenza, T. (2007). Genetic differentiation of an endangered capercaillie (*Tetrao urogallus*) population at the southern edge of the species range. *Conservation Genetics*, *8*(3), 659–670. https://doi.org/10.1007/s10592-006-9212-z

Rowan, B. A., Heavens, D., Feuerborn, T. R., Tock, A. J., Henderson, I. R., & Weigel, D. (2019). An ultra high-density *Arabidopsis thaliana* crossover map that refines the influences of structural variation and epigenetic features. *Genetics*, *213*, 771–787.

Saada, G., Nicastro, K. R., Jacinto, R., McQuaid, C. D., Serrão, E. A., Pearson, G. A., & Zardi, G. I. (2016). Taking the heat: Distinct vulnerability to thermal stress of central and threatened peripheral lineages of a marine macroalga. *Diversity and Distributions*, *22*(10), 1060–1068. https://doi.org/10.1111/ddi.12474

Sagarin, R. D., Ambrose, R. F., Becker, B. J., Engle, J. M., Kido, J., Lee, S. F., Miner, C. M., Murray, S. N., Raimondi, P. T., Richards, D., & Roe, C. (2007). Ecological impacts on the limpet *Lottia gigantea* populations: Human pressure over a broad scale on Island and mainland intertidal zones. *Marine Biology*, *150*(3), 399–413. https://doi.org/10.1007/s00227-006-0341-1

Sanford, E., Sones, J. L., García-Reyes, M., Goddard, J. H. R., & Largier, J. L. (2019). Widespread shifts in the coastal biota of northern California during the 2014–2016 marine heatwaves. *Scientific Reports*, *9*(1), 4216. https://doi.org/10.1038/s41598-019-40784-3

Sen Gupta, A., Thomsen, M., Benthuysen, J. A., Hobday, A. J., Oliver, E., Alexander, L. V., Burrows, M. T., Donat, M. G., Feng, M., Holbrook, N. J., Perkins-Kirkpatrick, S., Moore, P. J., Rodrigues, R. R., Scannell, H. A., Taschetto, A. S., Ummenhofer, C. C., Wernberg, T., & Smale, D. A. (2020). Drivers and impacts of the most extreme marine heatwave events. *Scientific Reports*, *10*(1), 19359. https://doi.org/10.1038/s41598-020-75445-3

Smith, K. A., Dowling, C. E., & Brown, J. (2019). Simmered then boiled: Multi-decadal poleward shift in distribution by a temperate fish accelerates during marine heatwave. *Frontiers in Marine Science*, *6*, 407. https://doi.org/10.3389/fmars.2019.00407

Stimson, J. (1970). Territorial behavior of the owl limpet. *Lottia Gigantea*. *Ecology*, *51*(1), 113–118. https://doi.org/10.2307/1933604

Sunday, J. M., Bates, A. E., & Dulvy, N. K. (2012). Thermal tolerance and the global redistribution of animals. *Nature Climate Change*, *2*(9), 686–690. https://doi.org/10.1038/nclimate1539

Szűcs, M., Vercken, E., Bitume, E. V., & Hufbauer, R. A. (2019). The implications of rapid eco-evolutionary processes for biological control—A review. *Entomologia Experimentalis et Applicata*, *167*(7), 598–615. https://doi.org/10.1111/eea.12807

Thompson, L. M., Thurman, L. L., Cook, C. N., Beever, E. A., Sgrò, C. M., Battles, A., Botero, C. A., Gross, J. E., Hall, K. R., Hendry, A. P., Hoffmann, A. A., Hoving, C., LeDee, O. E., Mengelt, C., Nicotra, A. B., Niver, R. A., Pérez-Jvostov, F., Quiñones, R. M., Schuurman, G. W., … Whiteley, A. (2023). Connecting research and practice to enhance the evolutionary potential of species under climate change. *Conservation Science and Practice*, *5*(2), e12855. https://doi.org/10.1111/csp2.12855

Thuiller, W., Albert, C., Araújo, M. B., Berry, P. M., Cabeza, M., Guisan, A., Hickler, T., Midgley, G. F., Paterson, J., Schurr, F. M., Sykes, M. T., & Zimmermann, N. E. (2008). Predicting global change impacts on plant species' distributions: Future challenges. *Perspectives in Plant Ecology, Evolution and Systematics*, *9*(3), 137–152. https://doi.org/10.1016/j.ppees.2007.09.004

Vieira, F. G., Albrechtsen, A., & Nielsen, R. (2016). Estimating IBD tracts from low coverage NGS data. *Bioinformatics*, *32*(14), 2096–2102. https://doi.org/10.1093/bioinformatics/btw212

Waltari, E., & Hickerson, M. J. (2013). Late Pleistocene species distribution modelling of North Atlantic intertidal invertebrates. *Journal of Biogeography*, *40*(2), 249–260. https://doi.org/10.1111/j.1365-2699.2012.02782.x

Wang, J., Cheng, Z.-Y., & Dong, Y.-W. (2022). Demographic, physiological and genetic factors linked to the poleward range expansion of the snail *Nerita yoldii* along the shoreline of China. *Molecular Ecology*, *31*(17), 4510–4526. https://doi.org/10.1111/mec.16610

Wares, J. P., Gaines, S. D., & Cunningham, C. W. (2001). A comparative study of asymmetrics migration events across a marine biogeographic boundary. *Evolution*, *55*(2), 295–306. https://doi.org/10.1111/j.0014-3820.2001.tb01294.x

Watterson, G. A. (1975). On the number of segregating sites in genetical models without recombination. *Theoretical Population Biology*, *7*(2), 256–276. https://doi.org/10.1016/0040-5809(75)90020-9

Weber, E. D., Auth, T. D., Baumann-Pickering, S., Baumgartner, T. R., Bjorkstedt, E. P., Bograd, S. J., Burke, B. J., Cadena-Ramírez, J. L., Daly, E. A., de la Cruz, M., Dewar, H., Field, J. C., Fisher, J. L., Giddings, A., Goericke, R., Gomez-Ocampo, E., Gomez-Valdes, J., Hazen, E. L., Hildebrand, J., … Zeman, S. M. (2021). State of the California current 2019–2020: Back to the future with marine heatwaves? *Frontiers in Marine Science*, *8*, 709454. https://doi.org/10.3389/fmars.2021.709454

Weersing, K., & Toonen, R. (2009). Population genetics, larval dispersal, and connectivity in marine systems. *Marine Ecology Progress Series*, *393*, 1–12. https://doi.org/10.3354/meps08287

Wei, X., Li, K., Kilpatrick, T., Wang, M., & Xie, S. (2021). Large-scale conditions for the record-setting Southern California marine heatwave of August 2018. *Geophysical Research Letters*, *48*(7), e2020GL091803. https://doi.org/10.1029/2020GL091803

Wilde, B. C., Rutherford, S., Yap, J.-Y. S., & Rossetto, M. (2021). Allele surfing and Holocene expansion of an Australian fig (Ficus—Moraceae). *Diversity*, *13*(6), 250. https://doi.org/10.3390/d13060250

Williams, J. L., Hufbauer, R. A., & Miller, T. E. X. (2019). How evolution modifies the variability of range expansion. *Trends in Ecology & Evolution*, *34*(10), 903–913. https://doi.org/10.1016/j.tree.2019.05.012

Zarzyczny, K. M., Hellberg, M. E., Lugli, E. B., MacLean, M., Paz-García, D. A., Rius, M., Ross, E. G., Treviño Balandra, E. X., Vanstone, J., Williams, S. T., & Fenberg, P. B. (2024). Opposing genetic patterns of range shifting temperate and tropical gastropods in an area undergoing tropicalisation. *Journal of Biogeography*, *51*(2), 246–262. https://doi.org/10.1111/jbi.14744

Zaytsev, O., Cervantes-Duarte, R., Montante, O., & Gallegos-Garcia, A. (2003). Coastal upwelling activity on the Pacific shelf of the Baja California peninsula. *Journal of Oceanography*, *59*(4), 489–502.

SUPPORTING INFORMATION

Additional supporting information can be found online in the Supporting Information section at the end of this article.

How to cite this article: Nielsen, E. S., Walkes, S., Sones, J. L., Fenberg, P. B., Paz-García, D. A., Cameron, B. B., Grosberg, R. K., Sanford, E., & Bay, R. A. (2024). Pushed waves, trailing edges, and extreme events: Eco-evolutionary dynamics of a geographic range shift in the owl limpet, *Lottia gigantea*. *Global Change Biology*, *30*, e17414. https://doi.org/10.1111/gcb.17414